4 Dispersive kinetics

Andrzej Plonka

Institute of Applied Radiation Chemistry, Wroblewskiego 15, 93-590 Lodz, Poland. E-mail: anplonka@cksg.p.lodz.pl

1 Introduction

Chemical reactions proceeding on time-scales comparable to or shorter than those of internal rearrangements in the reaction system renewing the environment of reactants (mixing) are, in general, dispersive. For dispersive kinetics, as for dispersive transport and dispersive relaxation,[1] many time-scales coexist, and the rate coefficients, termed the specific reaction rates, depend on time.[2,3]

In classical kinetics, the concept of an energy profile along a reaction path helps one to visualize the main features of a chemical reaction, including its mechanism. Along the reaction path, the reactants are separated from the products by a potential energy barrier. Specific reaction rates are related to thermally activated over-barrier transitions or to quantum-mechanical tunneling through the barrier. For a constant specific reaction rate a single potential energy barrier is envisaged for the whole reaction course. For a time-dependent specific reaction rate the potential energy barrier separating the reactants from products has to evolve during the reaction course. Since the first half of the last century there have been many studies aimed toward a mathematical description of barrier crossing processes in condensed-phase systems. When the time-scale of the environmental fluctuations is short compared to the time of the overall rate processes, the effect of the environments on the barrier crossing is merely to 'renormalize' the rate coefficient. However, there are many cases, such as electron transfer in viscous solvents, reactions of biomolecules, reaction in glasses and femtosecond events in fluid environments, where the fluctuations of the environment are slower than or comparable in time-scale to the overall barrier crossing. In this situation the traditional theory of chemical kinetics breaks down and we enter the vast areas of dispersive kinetics.[4–7]

In Section 2 some recent discussions on the basic concepts of kinetics and the common features of dispersive rate processes in condensed media are presented. Approximation of classical kinetics is discussed in Section 3. The extent to which the models of dispersive kinetics and the approximation of classical kinetics conform to reality is determined by testing them against experimental data. This is done in Section 4. Conclusions comprising Section 5 reflect to some extent the author's personal point of view and interest, which undoubtedly may be seen also in the choice of the subject matter from this rapidly developing interdisciplinary field of research.

DOI: 10.1039/b100666p

2 Phenomenological approach to dispersive kinetics

In dispersive kinetics one has to account for the distribution in reactivity of reactants. To illustrate the thesis that the distribution in reactivity is only seen when not preserved during the reaction course it seems highly instructive to consider the simple example of two states of the reactant, A_1 and A_2, giving the product P according to the simple kinetic scheme:

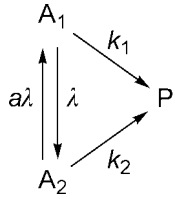

For this reaction scheme, the solution of the pair of simultaneous differential equations

$$-\frac{\mathrm{d}A_1}{\mathrm{d}t} = (k_1 + \lambda)A_1 - a\lambda A_2 \tag{1}$$

$$-\frac{\mathrm{d}A_2}{\mathrm{d}t} = (k_2 + a\lambda)A_2 - \lambda A_1 \tag{2}$$

is

$$A_1(t) = \frac{aA}{(1+a)(\gamma_1 - \gamma_2)}\left[(k_1 - \gamma_2)\exp(-\gamma_1 t) + (\gamma_1 - k_1)\exp(-\gamma_2 t)\right] \tag{3}$$

$$A_2(t) = \frac{A}{(1+a)(\gamma_1 - \gamma_2)}\left[(k_2 - \gamma_2)\exp(-\gamma_1 t) + (\gamma_1 - k_2)\exp(-\gamma_2 t)\right] \tag{4}$$

where

$$A = A_1(0) + A_2(0) \tag{5}$$

and γ_1 and γ_2 are negative roots of the algebraic equation

$$x^2 + (k_1 + k_2 + \lambda + a\lambda)x + k_2\lambda + k_1(k_2 + a\lambda) = 0 \tag{6}$$

equal to

$$\gamma_1 = \tfrac{1}{2}\left\{ k_1 + k_2 + \lambda + a\lambda + \sqrt{(k_1 + k_2 + \lambda + a\lambda)^2 - 4[k_2\lambda + k_1(k_2 + a\lambda)]}\right\} \tag{7}$$

$$\gamma_2 = \tfrac{1}{2}\left\{ k_1 + k_2 + \lambda + a\lambda - \sqrt{(k_1 + k_2 + \lambda + a\lambda)^2 - 4[k_2\lambda + k_1(k_2 + a\lambda)]}\right\} \tag{8}$$

For

$$A(t) = A_1(t) + A_2(t) \tag{9}$$

one gets

$$A(t) = \frac{A}{(1+a)(\gamma_1 - \gamma_2)} \times \left\{ \left[ak_1 + k_2 - (1+a)\gamma_2\right] \exp(-\gamma_1 t) - \left[ak_1 + k_2 - (1+a)\gamma_1\right] \exp(-\gamma_2 t) \right\} \quad (10)$$

or

$$A(t) = A\left[\eta \exp(-\gamma_1 t) + (1-\eta) \exp(-\gamma_2 t)\right] \quad (11)$$

where

$$\eta = \frac{ak_1 + k_2 - (1+a)\gamma_2}{(1+a)(\gamma_1 - \gamma_2)} \quad (12)$$

For equal rates of transition between the states 1 and 2, *i.e.* for α, γ_1 and γ_2 reduce to γ_1' and γ_2' given by

$$\gamma_1' = \tfrac{1}{2}\left[k_1 + k_2 + 2\lambda + \sqrt{(k_1 - k_2)^2 + 4\lambda^2} \right] \quad (13)$$

$$\gamma_2' = \tfrac{1}{2}\left[k_1 + k_2 + 2\lambda - \sqrt{(k_1 - k_2)^2 + 4\lambda^2} \right] \quad (14)$$

and η yields η' equal to

$$\eta' = \frac{k_1 + k_2 - 2\gamma_2'}{2(\gamma_1' - \gamma_2')} \quad (15)$$

Solution for this particular case was presented and discussed recently by Goldanskii *et al.*[8,9] It was shown that for $\lambda \gg k_1, k_2$, in our notation,

$$A(t) = A \exp\left[-\tfrac{1}{2}(k_1 + k_2)t\right] \quad (16)$$

which follows from $\eta' \rightarrow 0$ and $\gamma_2' = 1/2\ (k_1 + k_2)$ under this condition. It was also shown that for $\lambda \rightarrow 0$

$$A(t) = (A/2)\left[\exp(-k_1 t) + \exp(-k_2 t)\right] \quad (17)$$

which results from $\eta' = 1/2$ and $\gamma_1' = k_1$ and $\gamma_2' = k_2$ in this case. For the more general case, considered presently, of unequal rates of transitions between the states 1 and 2, the solution was not shown. The authors restricted their attention to discussing the most interesting special limiting cases corresponding to eqns. (16) and (17). Here these special cases are shown to follow from the general solution, eqn. (11).

The first case is when the relaxation rate is high compared to the reaction rate, *i.e.* $\lambda \gg k_1, k_2$. Instant relaxation of the matrix to the stationary distribution of states occurs. Under this condition $\eta \rightarrow 0$ and $\gamma_2 \rightarrow 0$ and $\gamma_2 \rightarrow ak_1/(1+a) + k_2/(1+a)$, which yields, *cf.* eqn. (11),

$$A(t) = A \exp\left[-\left(\frac{a}{1+a} k_1 + \frac{1}{1+a} k_2 \right) t \right] \quad (18)$$

i.e. monoexponential decay with the specific reaction rate equal to the weighted mean of the specific reaction rates for states 1 and 2.

The second case is when relaxation is much slower than chemical reactions. No relaxation of the matrix occurs during the time of conversion of the reagent. In our

notation $\lambda \rightarrow 0$ and from eqns. (7) and (8), respectively, $\gamma_1 = k_1$ and $\gamma_2 = k_2$; furthermore, from eqn. (12) $\eta = a/(1 + a)$, which yields, *cf.* eqn. (11),

$$A(t) = A\left[\frac{a}{1+a}\exp(-k_1 t) + \frac{1}{1+a}\exp(-k_2 t)\right] \tag{19}$$

i.e. biexponential decay. For illustrative example see Fig. 1.

It is easy to generalize eqns. (18) and (19), *cf.* Plonka,[2] for a given large number of states or to use a continuous distribution of states. It is hard to generalize and use eqn. (11) effectively. Instead, the stochastic model of reaction kinetics in renewing environments is explored.

Reaction kinetics in renewing environments

We have to recall that, in the stochastic model of reaction kinetics in renewing environments,[10] the structural reorganization of the host matrix is included by imposing upon the static disorder model the additional assumption that reinitialization occurs at random instants. The reinitialization consists of random reassignment of guest hopping rates with values having the same initial distribution.

Without renewals, in the three-dimensional disordered system, the number of distinct sites, $S(t)$, visited by a random walker was taken to be sublinear in time

$$S(t) = (t/\zeta_\alpha)^\alpha, \qquad 0 < \alpha < 1 \tag{20}$$

where ζ_α is the scaling time and α is the dispersion parameter.

Renewals are described by the fractal set of renewal moments following from the use of the Kohlrausch function

$$\Phi(t) = \exp[-(t/\tau_\beta)^\beta], \qquad 0 < \beta \leq 1 \tag{21}$$

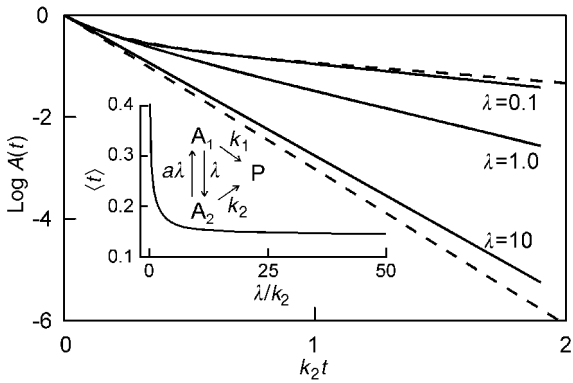

Fig. 1 Two-state kinetics. The solid curves depict the decay in time of $A(t)$ according to eqn. (11) for $k_1/k_2 = 10$, $a = 2$ and $\lambda = 0.1$, 1 and 10. The asymptotes, eqns. (18) and (19), are depicted by dashed lines. The inset shows the changes of the mean lifetime for A with λ.

to describe the internal rearrangements in the system. In eqn. (21), τ_β denotes the effective relaxation time and β is the dispersion parameter for relaxation.

Averaging $S(t)$ given by eqn. (20) over the renewal sequences following from relation (21), one gets[10]

$$\langle S(t)\rangle = (t/\hat{\zeta}_{\hat{\alpha}})^{\hat{\alpha}} \tag{22}$$

with

$$\hat{\alpha} = 1-(1-\alpha)(1-\beta) \tag{23}$$

$$\hat{\zeta}_{\hat{\alpha}} = \zeta_\alpha^{\alpha/\hat{\alpha}} \tau_\beta^{(1-\alpha/\hat{\alpha})} \tag{24}$$

For highly reactive species, for which the local reaction probability (when two reactants collide) is equal to unity, the specific reaction rate was taken as

$$k(t) = b\,\frac{\mathrm{d}\langle S(t)\rangle}{\mathrm{d}t} \tag{25}$$

where b denotes the volume of a site (cell) visited by the random walker. From eqns. (22) and (25) one gets for $k(t)$

$$k(t)/\mathrm{dm}^3\ \mathrm{mol}^{-1} = (\hat{\alpha}/\hat{\zeta}_{\hat{\alpha}})(t/\hat{\zeta}_{\hat{\alpha}})^{\hat{\alpha}-1} \tag{26}$$

It was shown[2] that, when the rate of chemical reaction markedly exceeds the rates of internal rearrangements, $1/\zeta_\alpha \gg 1/\tau_\beta$, then formally $\beta = 0$, and, *cf.* eqn. (23), $\hat{\alpha} = \alpha$, which is the case of a highly dispersive reaction pattern. If, on the other hand, the rates of internal rearrangements markedly exceed the rate of chemical reaction, $1/\tau_\beta \gg 1/\zeta_\alpha$, then $\beta = 1$, and, *cf.* eqn. (23), $\hat{\alpha} = 1$, which is the case of a classical reaction pattern. For further improvement of renewal arguments see Sokolov and Blumen.[11] See also Svare *et al.*[12] for the temperature dependence of β, Das and Srivastava[13] for a discussion of relaxation exponents over various time-scales, and Ross and Vlad[14] for a more general discussion of the effect of a disordered system on a chemical reaction in terms of environmental fluctuations.

Microscopic correlation-function expressions for the stochastic evolution observed in single-molecule spectroscopy were derived by Chernyak *et al.*[15] The kinetics of a multilevel quantum system coupled to a single collective overdamped Brownian-oscillator coordinate is exactly mapped onto a continuous-time random walk (CTRW) involving the transition states. Classified expressions are derived for the stochastic trajectories and the non-Poissonian distribution of number of flips. When the oscillator relaxation is fast compared with the reaction rates, the waiting time distribution becomes exponential and the standard Poisson kinetics is recovered. See also Kuno *et al.*[16] for a universal power-law behavior in non-exponential 'blinking' kinetics of single CdSe quantum dots. It is stressed[16] that, since its inception in 1989, single-molecule spectroscopy has made significant progress towards elucidating the photophysics of isolated species in the absence of ensemble averaging. Motivations for such single-molecule studies include identifying individual contributions to the ensemble averaging and understanding interactions with its environment. Quantum dots are low-dimensional materials and are therefore interesting from both fundamental and applied viewpoints. From a fundamental perspective, quantum dots

represent an intermediate stage between a single molecule and the condensed phase, and consequently allow one to study the evolution of bulk properties with sample size. Practical interest in these materials arises from applications ranging from nanoscale electronics to biological fluorescent labeling.

For a discussion of the fractional power dependence of the mean lifetime of a first-order reaction on a time-scale of the environment relaxation, see Okada.[17]

Temperature dependence of rate parameters

It was recalled by Logan[18] that in one of his papers from 1887 Arrhenius had put in a plea for the adoption of the term 'specific reaction rate' rather than 'rate constant' on the grounds that this parameter was not invariant. Had his view prevailed it would have obviated the use of the apparently self-contradictory term, 'time-dependent rate constant', which arose in connection with the behavior of pairs of reactive entities produced in close proximity in solution[19] and, of course, in the dispersive kinetics.

Logan[18] quotes the classic paper of Arrhenius[20] which appeared in 1889 under the title 'Über die Reaktionsgeschwindigkeit bei der Inversion von Rohrzucker durch Säuren'. In the first section, Arrhenius considered eight sets of published data on the effect of temperature on reaction rates and showed (using more currently conventional symbols) that in each case he could choose a value of the constant C such that $k(T_1)$, the rate constant at temperature T_1, was represented adequately by the equation

$$k(T_1) = k(T_0)\exp[C(T_1 - T_0)/T_1T_0] \tag{27}$$

where T_1 and T_0 are the relevant temperatures. This was tantamount to showing that the rate constant could be represented as an explicit function of temperature, namely

$$k(T) = A\exp(-C/T) \tag{28}$$

where $A = k(T_0)\exp(C/T_0)$ and both A and C are constants for the particular reaction.

Discussing this in relation to the inversion of sucrose, Arrhenius proposed[20] that the actual substance with which acids reacted to bring about the inversion process was not simple cane sugar but a substance 'active cane sugar' which, to use more contemporary terminology, he envisaged as being a tautomeric form of ordinary 'inactive' cane sugar, formed endothermically from it and in rapid equilibrium with it. Thus, using the van't Hoff reaction isochore, he deduced the equation

$$\frac{\mathrm{d}\ln k(T)}{\mathrm{d}T} = \frac{q}{RT^2} \tag{29}$$

where q represented what would now be called the standard molar enthalpy of the 'active' form less that of the much more abundant 'inactive' tautomer. (A further implicit assumption made here was that the rate of reaction of the "active" form did not vary with temperature.) Thus the empirical constant C in eqns. (27) and (28), with the dimension of reciprocal temperature, was equated to q/R, where q has the dimension of energy per mole.

Although this reaction model did not hold sway for long, as there evolved the more familiar expression for the Arrhenius equation

$$k(T) = A \exp(-E_a / RT) \tag{30}$$

the constant E_a was labeled the 'action energy' on the historical basis that it represented, in the Arrhenius model, the energy required to convert the reacting substance into the 'active' form.

It is now accepted that although, over a limited range of temperature, plots of $\ln k(T)$ against T^{-1} are acceptably linear and may quite reasonably be used for the purposes of interpolation, eqn. (30) is not in general obeyed, even by elementary chemical reactions, in the sense that unique constants A and E_a do not exist for each reaction. Thus, it is now recognized that, even when the Arrhenius plot is apparently linear, E_a is best regarded as an empirical or phenomenological quantity, defined as

$$E_a = -R \frac{\mathrm{d} \ln k(T)}{\mathrm{d}(1/T)} \tag{31}$$

and, to minimize misunderstandings, termed 'the Arrhenius activation energy'. Logan[18] concludes that in many instances E_a is a quantity with no (not even approximate) physical significance. Others were less pessimistic, *cf.* the previous report.[7]

The actual obstacle to interpretation of experimentally determined values of E_a and A lies in the nature of experiments. The experimental techniques do not provide the complete isolation of the elementary reaction (nucleation, nuclei growth) uncomplicated by diffusion, adsorption, desorption and other physical processes. In other words, experimental techniques used in solid-state kinetics generally do not measure the reaction rates of elementary steps but instead measure the overall rate of a process which usually involves several steps with different activation energies. For this reason, experimentally derived Arrhenius parameters of a solid-state process tend to have an overall (effective) nature. By virtue of their effective nature, Arrhenius parameters of solid-state reactions are difficult to interpret in terms of the transition-state theory. Therefore, a sound way to settle the issue of the applicability of the Arrhenius equation is to use it and to treat computed Arrhenius parameters as effective constants unless mechanistic conclusions are justified by auxiliary data. See also Marsi and Seres,[21] Urbanovici *et al.*,[22] Wilburn,[23] Ozawa[24,25] and Suga.[26]

As recalled by Nakamura *et al.*,[27] the Arrhenius equation cannot be extended to extremely low temperatures, because the quantum states of any reactant molecules and radicals at extremely low temperatures are confined to their ground states from which reactions occur through tunneling. He has proposed a modified Arrhenius equation

$$k(T) = A \exp\left(-\frac{E_a}{R\sqrt{T^2 + T_0^2}} \right) \tag{32}$$

where T_0 is an additional constant. If we denote by r the ratio of the rate constant taking into account quantum-mechanical tunneling to that ignoring the contribution of quantum tunneling, *i.e.*

$$r = \exp\left(-\frac{E_a}{R\sqrt{T^2 + T_0^2}} \right) \Big/ \exp\left(-\frac{E_a}{RT} \right) \tag{33}$$

then the contribution of tunneling in the total reaction may be calculated by

$$\eta = (r-1)/r \tag{34}$$

A number of results presented suggest that (1) most organic reactions, in which the transfer of H, H^+, or H^- is often the rate-determining step, mainly occur through tunneling even at room temperature, and (2) the potential barrier heights estimated by the *ab initio* calculations are probably 20–30% higher than the activation energies of these reactions experimentally determined at around room temperature.

Talking about extension of the Arrhenius equation to low temperatures we have to remember, however, that we have $k(t)$ not k. Furthermore, $\langle k(t) \rangle = \infty$. As an example, Barkatt *et al.*[28] have measured the recombination of the charge pairs NO_3 and NO_3^{2-} in 3:2 KNO_3–$Ca(NO_3)_2$ glass from 77 to 486 K and 10^{-6} to 10^2 s for 4×10^{18} eV electron pulses by observing NO_3 at 615 nm. The decay patterns at high temperatures were fitted with a model developed for diffusion in the presence of an electrostatic field, *cf.* Rzad *et al.*,[29] which leads to the dependence

$$G(t) = G(0) \exp(\lambda t) \ \mathrm{erfc}(\lambda t)^{1/2} \tag{35}$$

where G denotes the radiation yield of charge pairs, per 100 eV, and λ, s^{-1}, is the ionic recombination parameter. This function, originally developed for the case of ion pair recombination in nonpolar liquids, was known to fit the results obtained in oxide glasses and in low-temperature aqueous glasses above the glass transition temperature.[30,31] In the case under discussion, deviations from eqn. (35) become larger as the temperature is lowered towards and below the glass transition temperature. Below 297 K the decays become nearly linear with the logarithm of time over a wide range of times. This behavior was thought[28] to be typical of tunneling reactions between species held at fixed distances when diffusion is frozen out. The very wide range of recombination times results mainly from the strong, exponential dependence of the tunneling rate on distance, *cf.* eqn. (97) below. These reactions are temperature-dependent, even well below the glass transition temperature, where diffusion cannot be invoked. The Arrhenius plots could not be constructed in an unambiguous way mainly because of the complex nature of the kinetics. Barkatt *et al.*[28] have plotted the reciprocals of the times necessary to decay to two-thirds and one-third of the 'initial' absorbance, assumed to be equal at all temperatures to the absorbance at 1 μs at a temperature of 77 K. For thus constructed Arrhenius plots the most striking feature is their decided nonlinearity. The exact shapes of the true Arrhenius plots were uncertain, but it was clear that the activation energy is small at low temperatures, about 3 kcal mol^{-1}, and larger at higher temperatures, about 20 kcal mol^{-1}.

Hamill[32] assumed the prolonged decay, with $G(NO_3)$ roughly linear with the logarithm of time, to be quantitatively consistent with dispersive hole hopping by electron transfer from NO_3^- to NO_3. Expecting second-order kinetics with $k(t)$, the purpose was to examine the applicability of the equation

$$1/G - 1/G_0 = (B/\alpha)t^{\alpha} \tag{36}$$

to recombination kinetics in nitrate ion glass as a simple model system and to consider the temperature dependence. The results of his test are depicted in the inset in Fig. 2, for $G_0 = 4.3$. No Arrhenius plot was constructed. The lines in the inset in Fig. 2 were claimed to converge at 10^{-13} s. Therefore for $k(t)$ in the form

$$k(t) = A_0(t/\tau)^{\alpha-1} \exp(-E_0/kT) \tag{37}$$

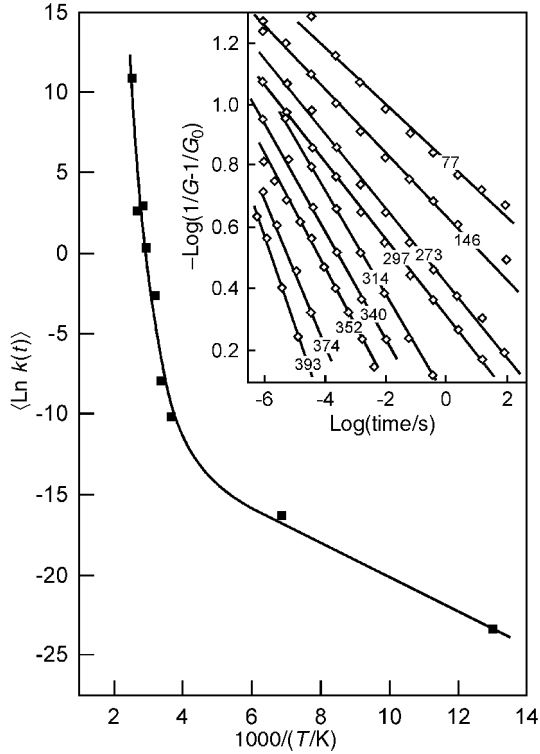

Fig. 2 Analysis of data of Barkatt *et al.*[28] on recombination of charge pairs in 3:2 KNO_3–$Ca(NO_3)_2$ glass. Details in text.

one has $\tau = 10^{-13}$ s, $E_0 = 0$ and A_0 independent of temperature. Activation energy changes with time according to

$$E(t) = E_0 + (1-\alpha)kT\ \ln(t/\tau) \tag{38}$$

Reported are the values of E(1 s), changing from 0.18 eV ($\sim$ 4 kcal mol^{-1}) at 77 K to 0.72 eV ($\sim$ 17 kcal mole^{-1}) in the temperature range 340–393 K.

There is no mean value of $\langle k(t)\rangle$ for the reaction course. There is, however, the mean value of the logarithm of $k(t)$, $\langle \ln k(t)\rangle$, given by, *cf.* eqn. (26) for $\tau \equiv \zeta_{\hat{\alpha}}$ and $\hat{\alpha} \equiv \alpha$,

$$\langle \ln k(t)\rangle = \ln(\alpha/\tau) + (\alpha - 1)\langle \ln(t/\tau)\rangle \tag{39}$$

For the second-order equal-concentration kinetics, *cf.* Box 2 below, for $\tau \equiv \alpha_{\hat{\alpha}}$ and $\alpha \equiv \hat{\alpha}$, $\langle \ln(t/\tau)\rangle = 0$, and therefore

$$\langle \ln\ k(t)\rangle = \ln(\alpha/\tau) \tag{40}$$

or

$$\langle \ln\ k(t)\rangle = \ln[\alpha(B/\alpha)^{1/\alpha}] \tag{41}$$

for the notation used in eqn. (36).

Using the tabulated values,[32] the Arrhenius plot presented in Fig. 2 was constructed. From this plot, the mean activation energy $\langle E(t) \rangle$ changes from 2.3 kcal mol^{-1} (0.10 eV) in the low-temperature region to 53.0 kcal mol^{-1} (2.3 eV) in the high-temperature region.

Rate constants for several reactions have been measured over a temperature range exceeding 1000 K, with the largest class being gas-phase hydrogen abstraction by radicals, *cf.* Zavitsas.[33] Over extended temperature ranges, the experimental data are often described by the three-parameter equation

$$k = aT^n \exp(-b/RT) \tag{42}$$

Curvatures of Arrhenius plots for different reactions vary widely, from minimal [$n \sim 0$, in eqn. (42)] to quite pronounced ($n = 6$). For $n = 1$, eqn. (42) is equivalent to that following from Eyring's transition-state theory

$$k = \kappa(k_B/h)T \exp(\Delta S^{\ddagger}/R) \exp(-\Delta H^{\ddagger}/RT) \tag{43}$$

where k_B and h are the Boltzmann and Planck constants and $\Delta S^{\ddagger}$ and $\Delta H^{\ddagger}$ are the entropy and enthalpy of activation, respectively. For some recent extensions of Kramers[34] approach see *e.g.* Berezhkovskii *et al.*,[35] Chaudhuri *et al.*,[36] and Banik *et al.*[37]

The Williams–Landel–Ferry (WLF)[38] equation is one of the best-known equations of polymer physics, and for a long time it was believed to describe an almost universal non-Arrhenius effect of temperature on viscosities and relaxation times in polymer systems. The equation is written as

$$\begin{aligned} \log a_T &= \log[\tau(T)/\tau(T^*)] \\ &= C_1(T - T^*)/[T - (T^* - C_2)] \end{aligned} \tag{44}$$

where a_T is called the shift factor, $\tau(T)$ is the relaxation time at temperature T, $\tau(T^*)$ is the relaxation time at some reference temperature T^* within the range of measurement, and C_1 and C_2 are constants. When the measurement range includes the glass transition temperature T_g (from calorimetry or dilatometry), it has been natural to choose T_g as the reference temperature T^*. When T_g was defined in some consistent way by measurement of thermal or volumetric changes at a fixed scan rate, usually $\sim$ 1 K min^{-1}, then the parameters C_1^g and C_2^g appeared to have universal values.[39]

For simple liquids and oxide melts, deviations from Arrhenius temperature dependence have most commonly been described by the well-known Vogel–Tammann–Fulcher (VTF) equation,[6] which is exemplified by

$$\eta = \eta_0 \exp[B/(T - T_0)] \tag{45}$$

or

$$\tau = \tau_0 \exp[B/(T - T_0)] \tag{46}$$

Here η is the viscosity, τ is a relaxation time, and η_0, τ_0, B and T_0 are constants. The success of this equation for simple liquids seemed to be comparable with that of the WLF equation for polymers.

As discussed by Rault[40] all glass-forming materials, simple liquids and polymers show the α–β bifurcation; above a cross-over temperature T^*, the glass α transition and the β secondary transition merge together. Below this bifurcation temperature the

relaxation times τ and τ_β of the cooperative (α) and non-cooperative (β) movements verify, respectively, the Vogel–Fulcher–Tammann (VFT) and Arrhenius laws. This temperature is of the order of $1.3T_g$ and in crystallizable materials T^* is found to be equal to the melting temperature; the frequency of the α and β motions at that temperature is of the order of 10^7–10^9 s^{-1} depending on the nature of the material. In the domain $T_g < T < T_g + 100$ °C the cooperativity parameter n (Kohlrausch exponent) of the α movements is of the form

$$n = (T - T_0)/(T^* - T_0)$$

where T_0 is a temperature below T_g where the relaxation time τ_0 and the exponent n extrapolate, respectively, to infinity and to zero. When the characteristic temperatures T^* and T_0 increase linearly with pressure, then n at constant temperature is also a decreasing function of pressure; $1/n$ can be considered as the number of individual units (of β type) participating in the α motion, and therefore the relaxation time τ verifies the power law

$$\tau = \tau_0(\tau_\beta / \tau_0)^{1/n}$$

between T_0 and T^*, τ_0 being the phonon frequency and τ_β the frequency of the β movements. This equation is not very different from the Ngai relation concerning the relaxation time of complex systems, *cf.* eqn. (75) and the meaning of the parameter n in both cases. Combining both relations $n \sim T$ and $\tau \sim \tau_\beta^{1/n}$, one finds that the relaxation time is given by the relation

$$\log(\tau / \tau_0) \approx A / T(T - T_0)$$

with $A = E_\beta(T^* - T_0)/2.3R$, E_β being the activation energy of the β motions. This law, called the modified VFT law, fits the experimental results better than the other phenomenological or theoretical models. This law, without an adjustable parameter, is compared to the VFT law obtained if one assumes that the cooperativity parameter n varies as $-1/T$. The relationships between the fragility index, capacity jump and the n_g value at T_g are discussed.

Bendler *et al.*[41] have developed a model that describes dielectric relaxation, ionic conductivity and viscosity of glass-forming liquids near the glass transition temperature. The model is based on the theory of defect diffusion and predicts the effects of pressure and temperature on dynamical phenomena according to

$$\tau = \tau_0 \exp\left[\left(\frac{T_0}{T - T_0}\right)^{3/2} \frac{1}{(1 - \chi P)^3}\right] \tag{47}$$

where χ denotes the compressibility and P stands for pressure.

According to the Adam and Gibbs equation[42]

$$\tau = \tau_0 \exp\left[\frac{s_c^* \Delta\mu}{k_B T S_{conf}}\right] \tag{48}$$

where s_c^* is the critical entropy, $\Delta\mu$ is the energy barrier for reorientation of a monomer group in the Adam–Gibbs theory, k_B is the Boltzmann constant, and T is the temperature. The ratio, $(s_c^* \Delta\mu / k_B)$, is a constant denoted by C. Thus

$$\tau = \tau_0 \exp\left[\frac{C}{TS_{\text{conf}}}\right] \tag{49}$$

The configurational entropy of a liquid, S_{conf}, decreases on cooling and it is expected to become zero for an equilibrium liquid at a temperature above 0 K. Therefore, according to eqn. (49), τ is expected to approach infinity. Adam and Gibbs used this decrease in S_{conf} to explain why the temperature dependence of the viscosity and τ of a supercooled liquid was non-Arrhenius, and why it followed the Vogel–Fulcher–Tammann type behavior.

In eqn. (49), neither S_{conf} nor C can be determined by experiments. Therefore, the value of τ_0 in eqn. (49) cannot be deduced from the τ data measured at different temperatures. For this reason, eqn. (49) has been combined with the Vogel–Fulcher–Tammann equation (46), where $A_{\text{VFT}} \equiv \tau_0$, B and T_0 are empirical constants, and all three can be determined from the known variation of τ with temperature. On that assumption, *cf.* eqn. (49), the quantity S_{conf} becomes related to τ by

$$S_{\text{conf}} = \frac{C}{T(\ln \tau - \ln A_{\text{VFT}})} \tag{50}$$

To test the validity of eqn. (49) and (50), it is still required that S_{conf} be known. It has been assumed that S_{conf} is the same as ΔS at T_g or at T close to T_g.

According to Huth *et al.*[43] the Adam–Gibbs paper,[42] one of the most cited works in physics, has a continuing influence on research into the glass transition. This paper is generally considered as the turning point from rare free volume to small configurational entropy as the reason for slow molecular mobility in glass formers. The reader, however, is confronted with a dilemma. The slowing down is conceptually linked with increasing cooperativity, but in fact we find only a formula to link mobility with configurational entropy. Neither the size of cooperativity nor its temperature dependence can be calculated from Adam–Gibbs formulas. Huth *et al.*[43] compare predicted temperature dependences of cooperativity for two post-Adam–Gibbs variants (the first *via* the configurational entropy and the second *via* a fluctuation approach) with the temperature dependence of cooperativities determined by means of heat capacity spectroscopy (HCS) data for polystyrene, polyisobutylene and a random copolymer (SBR 1500). The data yield a strong increase of cooperativity with lower temperature and, taking previous HCS data into account, indicate a cooperativity onset about 100 K above the Vogel temperature for these polymers. An acceptable fit of the cooperativity data can formally be reached by both post-Adam–Gibbs variants only upon the condition that this onset is included. The problem of a final decision between both variants and the conceptional differences between the configurational entropy approach and the fluctuation approach to glass transition are discussed. For application of the Adam–Gibbs equation to the non-equilibrium glassy state see Hutchinson *et al.*[44]

An analysis of the heat capacity data of 21 materials by Johari[45] shows that a glass loses 17–80% of its entropy on cooling from its T_g to 0 K, and that the entropy difference between a glass and crystal phase at T_g, $\Delta S(T_g)$, is 1.2–4.9 times the entropy difference at 0 K. This is contrary to the premise that the vibrational entropy of a glass is the same as the entropy of its crystal phase, or that $\Delta S(T_g)$ is equal to $S_{\text{conf}}(T_g)$, the configurational entropy at T_g. The excess entropy of a glass over the crystal phase is

attributed to (i) the relatively lower frequency and greater anharmonicity of lattice vibrations, which contribute to their vibrational entropy, (ii) the kinetically unfrozen modes corresponding to the tail of the distribution of the α-relaxation times, which contribute to the configurational entropy, and (iii) localized relaxations of molecular groups, which also contribute to the configurational entropy. These contributions vanish or become negligible at 0 K. Therefore, $\Delta S(T_g)$ cannot be used in place of $S_{conf}(T_g)$ in the Adam–Gibbs equation. An upper bound S_{conf} may be estimated at T_g by extrapolation of the vibrational entropy of a glass and used in the Adam–Gibbs equation to estimate roughly S_{conf} of a supercooled liquid from the dielectric relaxation time data.

Literature data on the entropy and heat capacity of 33 glass-forming liquids have been used by Johari[46] to examine the validity of the Adam–Gibbs relation between a liquid's configurational entropy, S_{conf}, and its molecular kinetics. The critical entropy, s_c^*, of $k_B \ln 2$ ($= 0.956 \times 10^{-23}$ J molecule^{-1} K^{-1}) in the equation is less than even the residual entropy per molecule in a glass at 0 K, and this creates difficulties in determining the size of the cooperativity rearranging region, z^*, in the liquid. It is argued that $z^* = [1 - (T_0/T)]^{-1}$, and the temperature-invariant energy term, $\Delta\mu$, is equal to RB, which has been determined from the knowledge of the Vogel–Fulcher–Tammann parameters B and T_0, with R being the gas constant, and on the basis of the argument that the pre-exponential term of this equation is identical to that of the Adam–Gibbs relation. As the lattice modes in a glass are lower in frequency and more anharmonic than in its crystal, its vibrational entropy, S_{vib}, would be higher than that of the crystal phase. Therefore, S_{conf} of a glass (and liquid) is significantly less than the difference between the entropy of the glass (and liquid) and the entropy of its completely ordered crystal phase. Both quantities, S_{vib} and S_{conf}, have been estimated without reference to the vibrational spectra. The conclusions can be tested by determining z^* and $\Delta\mu$ from measurements of the dielectric spectra of a liquid confined to nanometre-sized pores. This was elaborated by a calculation for 3-bromopentane.

In order to investigate whether the anomalous decrease in the net entropy of water on supercooling indicates a structural change, its entropy and relaxation time data have been examined by Johari[47] by equating the Adam–Gibbs expression with the Vogel–Fulcher–Tammann equation. This gave values of the minimum size of the cooperatively rearranging region as 4.7 molecules at 150 K, and the temperature-invariant energy as 7.42 kJ mol^{-1}. On the premise that a liquid's configurational entropy, S_{conf}, differs from its excess entropy over the ordered crystal state, S_{conf} of water has been estimated over the 150–273 K range by using the available value of its excess entropy at ~150 K. Water's S_{conf} at 273 K is found to be less than half of its entropy of fusion and to further decrease continuously on supercooling. This puts into question the conjecture that water structurally transforms near 228 K, as deduced by assuming that water's configurational entropy is equal to its excess entropy.

Finally Johari[48] stressed that, in our current discussion of the thermodynamics and molecular kinetics of glass-forming liquids, the entropy is extrapolated below a liquid's vitrification temperature T_g along a curve of progressively increasing slope until a temperature T_k is reached. Here the entropy and heat capacity, C_p, of the equilibrium liquid become equal to those of its crystal. Several observations have indicated fundamental difficulties with this extrapolation, thus suggesting the need for

an alternative. Johari[48] proposes an alternative, in which C_p of an equilibrium liquid decreases along a sigmoid-shaped path stretching over a broad temperature range from above T_g to 0 K. Its heat capacity C_p becomes equal to that of its crystal at 0 K, as required by the third law of thermodynamics, and the enthalpy and volume remain higher. To elaborate, the available C_p data of 12 supercooled liquids have been interpolated between $T > T_g$ and 0 K, and the enthalpy of their equilibrium state at 0 K, as well as the Gibbs free energy and enthalpy at $T < T_g$, determined. The enthalpy of the equilibrium liquid state at 0 K is 17–37% of the enthalpy of melting, and for eight out of 12 liquids the Kauzmann extrapolation and interpolation yield values within 5% of the average.

The deviation from Arrhenius behavior may be quantified by the parameter D in a modified form of eqn. (46), *i.e.*

$$\tau = \tau_0 \exp[DT_0/(T - T_0)] \tag{51}$$

where D is a 'strength' parameter, or by the fragility index, m, *cf.* Plonka,[6] *i.e.*

$$m = \left.\frac{\mathrm{d}\log\langle\tau\rangle}{\mathrm{d}(T_g/T)}\right|_{T=T_g} \tag{52}$$

A convenient parameterization of fragility would be $F = D^{-1}$, which varies between 0 and 1. An alternative parameterization related more closely to the WLF parameter, C_2, comes out of the analysis presented by Angell.[39] In theoretical efforts to account for the form of the VTF temperature dependence, τ_0 is seen as a microscopic quantity related to the frequency of attempts to cross some barrier opposing the rearrangement of particles involved in relaxation, or the time a molecule needs to move into some free space, and it is expected to have phonon-like time-scales, 10^{-14} s. The scaling temperature T_g was chosen as the temperature at which $\tau = 10^2$ s. The assignment is consistent with the common observation, usually by an extrapolation of eqn. (46), that $\tau_{\mathrm{dielectric}} = 10^2$ s (or $f_{\max} = 10^{-3}$ Hz) at the 10 K min^{-1} calorimetric T_g (onset definition).

The number of orders of magnitude between the relaxation time at T_g and the inverse attempt frequency (τ at $1/T = 0$) is ~16. From the temperature dependence of viscosity the corresponding number is 17. There is mathematical equivalence of the WLF and VTF equations. The well-known identities are, *cf.* Plonka,[6]

$$C_2 = T^* - T_0 \tag{53}$$

$$2.303 C_1 C_2 = B \tag{54}$$

Identification of C_1^g with $(\log \tau_g - \log \tau_0)$, hence with the number ~16, is shown from eqns. (46), (53) and (54) by simple algebra. Yet for reasons that are not very obvious, the relation

$$C_1^g = \log(\tau_g/\tau_0) \tag{55}$$

was overlooked for a long time. For viscosity, one obtains

$$C_1^g = \log(\eta_g/\eta_0) \tag{56}$$

Since τ_g has the value 10^2 s by assignment, the approximately universal value of $C_1^g = 17$ found empirically for 'well-behaved' polymers [implying τ_0 of eqns. (46) and

(51) equal to 10^{-14} s] can be seen as support within the polymer class of materials for the theoretical supposition that the VTF pre-exponent is a microscopic dynamical quantity, such as an inverse attempt frequency for barrier crossing. See also Johari.[49] For a discussion on the origin of the VTF equation near the liquid–glass transition see Kitamura,[50] and for the changes of conductivity behavior from Arrhenius to WLF type see Carvalho *et al.*[51]

Time-scale invariance of dispersive rate processes

Dispersive kinetics, like dispersive transport and relaxation, is time-scale-invariant, *cf.* the above-mentioned presentation by Scher *et al.*[1] of dispersive transport and relaxation, and the author's account of the early developments of dispersive chemical kinetics.[2]

In the familiar continuous-time random walk (CTRW) model, the time-scale invariance was attributed to the long-tailed distribution

$$\Psi(t) \sim t^{-\alpha-1} \tag{57}$$

of time between events that limit the motion. Then Hilfer and Anton,[52] *cf.* the previous report,[7] have shown that there is a precise and rigorous relation between the theory of continuous-time random walks and the fractional master equation, *i.e.* a master equation in which the time derivative is replaced with the derivative of fractional order. Comparison of the models exhibits the form of $\Psi(t)$,

$$\Psi(t;\omega,C) = \frac{t^{\omega-1}}{C} \sum_{k=0}^{\infty} \frac{1}{\Gamma(\omega k+\omega)} \left(-\frac{t^{\omega}}{C}\right)^{k} \tag{58}$$

The series in eqn. (58) was recognized as a generalized Mittag–Leffler[53] function, denoted as $E_{\omega,\omega}(x)$, and thus one has alternatively

$$\Psi(t;\omega,C) = \frac{t^{\omega-1}}{C} E_{\omega,\omega}\left(-\frac{t^{\omega}}{C}\right) \tag{59}$$

The series representation (58) shows that the waiting time density is a natural generalization of an exponential waiting time density to which it reduces for ω = 1,

$$\Psi(t;1,C) = (1/C)\ \exp(-t/C) \tag{60}$$

For $t \rightarrow 0$ one gets from eqn. (59)

$$\Psi(t) \sim t^{-1+\omega} \tag{61}$$

and for $t \rightarrow \infty$ and $0 < \omega < 1$

$$\Psi(t) \sim t^{-1-\omega} \tag{62}$$

i.e. an algebraic tail considered previously, *cf.* eqn. (57). The fractional order ω of the time derivative in eqn. (46) is restricted to $0 < \omega \leq 1$ as the result of the general theory, and special significance is attributed to the two limits $\omega \rightarrow 1$, *cf.* eqn. (60), and $\omega \rightarrow 0$, for which $\Psi(t) \rightarrow 1/t$. See also Barkai *et al.*[54–56] Recently fractional calculus is encountering much success in the description of complex dynamics, *cf.* Kusnezov *et al.*,[57] Rocco and West[58] and Schiessel *et al.*[59]

According to Zaslavsky,[60] short-memory dynamics is an important feature of the randomness that particles should obey. It was demonstrated, however, that physical processes do not satisfy the principle of short-memory randomness and that long power-like tails in distributions of different time-scales frequently occur in experimental systems. Long-tailed waiting time distributions give rise, *cf.* Metzler *et al.*,[61] to a time-fractional Fokker–Planck equation that describes systems close to equilibrium. Using this equation, for the force-free case, the subdiffusive behavior is recovered. The equation obeys the generalized Einstein relations and its stationary solution is the Boltzmann distribution. The relaxation of single modes follows a Mittag-Leffler decay, *cf.* Metzler *et al.*[62] and Metzler and Klafter.[63]

Sokolov[64] has recalled recently that the story of scaling concepts in turbulent flows started from the seminal work of Richardson,[65] who observed that the mean square relative separation between two particles, initially in close vicinity, evolves in time according to

$$R^2(t) = \left\langle r^2(t) \right\rangle \sim t^3 \tag{63}$$

Moreover, Richardson formulated a differential equation for the evolution of the distribution function of the two-particle distances, being of the form of a diffusion equation with the distance-dependent diffusion coefficient

$$K(r) \sim r^{4/3} \tag{64}$$

giving a heuristic picture of particle separation. The problem of correct statistical description of Richardson's dispersion was continuously attacked for more than 70 years. Sokolov[64] has considered the two-particle dispersion in a velocity field, where the relative two-point velocity scales according to

$$v^2(r) \sim r^{\alpha} \tag{65}$$

and the corresponding correlation time scales as

$$\tau(r) \sim r\beta \tag{66}$$

He has shown that for $\alpha/2 + \beta < 1$ the diffusion approximation holds, and the increase in the interparticle distances is governed by the distance-dependent diffusion coefficient

$$K(r) \sim r^{\alpha+\beta} \tag{67}$$

The possible regimes outside of the validity of the diffusion approximation are also discussed. See also Sokolov *et al.*[66,67] The anomalous behavior of the mean square displacement of hopping ions was investigated by Ishii[68] in a random lattice system by the relaxation model theory. It is made clear that its short-time behavior, which is linear in time *t*, is contributed to by localized non-diffusive modes, and the long-time behavior, also being linear in *t*, originates from the diffusive mode. In the intermediate time domain, two anomalous regions exist which are universally expressed by

$$\left\langle \Delta R(t)^2 \right\rangle \approx C't^{k'} + Ct^{k} \tag{68}$$

typically with $k' \approx 0$ and $k \approx 0.4$; the localized non-diffusive modes result in $C't^{k'}$ dominating the shorter-time region, while the extended non-diffusive modes govern the longer-time region of Ct^{k}. See also Schulzky *et al.*[69] for the similarity group and anomalous diffusion equations.

Non-exponential relaxation was one of the earliest studied and most often observed properties of condensed matter, *cf.* Chamberlin.[70] More than 130 years ago it was first recognized that the observed response from many diverse substances may exhibit two distinct types of non-exponential relaxation, and although the stretched exponential and Curie–von Schweidler power law have since been used to characterize the observed response from thousands of measurements, there is still no commonly accepted explanation for these empirical formulas. This raises the theoretical questions: why are there two types of non-exponential behavior, and why are they so 'universal'?

A general equation for the susceptibility of disordered systems was proposed by Bergman.[71] It is based on the experimental observation of power laws at frequencies far from the peak frequency of the imaginary part of the frequency-dependent relaxation function, the susceptibility. The obtained general expression contains the equations of other proposed relaxation functions as special cases and, thus, it might be considered as a generalization of these. From this general equation he derives an equation specially adapted for the α relaxation in glass-forming materials. This equation contains only three fitting parameters and it is thus very suitable for fitting real experimental data. It is shown that this equation is a good frequency domain representation of the time domain Kohlrausch stretched exponential. From the general equation he also derives a four-parameter 'universal' equation that describes most types of responses and even inverted response data, *i.e.* response peaks more stretched on the low-frequency side than on the (as is normal) high-frequency side. The physical significance of the different parameters is qualitatively discussed and the proposed functions are shown to satisfactorily describe typical experimental data. See also Govindaraj and Murugaraj.[72] For universality of ac conduction in disordered solids see Dyre and Schrøder,[73] and for ac conductivity dispersion in metaposphate glasses see Sidebottom.[74] See also Ishii and Abe.[75–77]

Although less common than the stretched exponential, the exponential with a fractal exponent bigger than unity has been encountered in spectroscopy and in the study of direct energy transfer in fractal systems with dynamic disorder, see also below. An apparently unrelated field in which the modified exponential law has been used is the study of life expectancy of humans in demography and health statistics, for instance, for the study of survival functions of cancer patients. To that we have added the survival statistics for microorganisms in a radiation field, *cf.* Plonka and Bogus.[78] In these fields both the stretched ($0 < \hat{\alpha} < 1$) and compressed ($\hat{\alpha} > 0$) exponentials have been used. It is easy to indicate further applications of compressed exponentials. The budding yeast *Saccharomyces cerevisiae* has a limited life span, defined by the number of times an individual cell divides. Life spans were determined for 43 individual cells by Jazwinski.[79] Buds were removed from 'mother' cells at maturity by micromanipulation and deposited in isolated spots on an agar slab. These 'virgin' cells that had never budded before were used to imitate the experiment. Every time the cell budded, the 'daughter' was removed at maturity and the 'mother' was scored one generation older, *cf.* inset in Fig. 3 depicting the cell spiral given in ref. 79. Fig. 3 presents the survival characteristics of *Saccharomyces cerevisiae* depicted from the numerical values reported by Jazwinski.[79] The solid line depicts the fit with a compressed exponential, with $\beta = 2.78 \pm 0.09$, *cf.* eqn. (21). See also the KJMA equation (126) below.

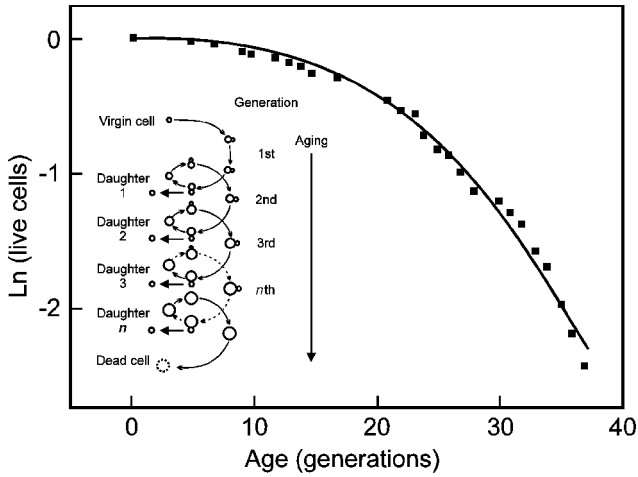

Fig. 3 Survival characteristics of *Saccharomyces cerevisiae*. Numerical data from Jazwinski.[79] Details in text.

The once abstract notions of fractal space and time now appear naturally and inevitably in chaotic dynamical systems and lead to *strange kinetics* and anomalous transport properties, *cf.* the previous report.[7] An understanding of this kind of dynamical behavior should provide insight into particle random walk processes, see Shlesinger *et al*.[80] Already the theory of dynamical chaos has changed the view of the possibility of statistical laws foundation, since dynamical trajectories, being the solutions of the deterministic equations of motion, may resemble curves representing random processes, see Zaslavsky.[81]

The phase space of a dynamical system is strongly non-uniform, *cf.* the previous report.[7] Within areas with chaotic dynamics there are islands which are not penetrated by the trajectories from the chaotic area. The borders of the islands are sticky, *i.e.* having arrived into a very narrow band at the border, the trajectory gets stuck there for a long time. This property of trajectories crucially influences the large-time-scale asymptotics for the survival time t_s, namely

$$t_s \equiv \int_0^\infty \tau\, \Psi_s(\tau)\, \mathrm{d}t \approx \int_0^{\text{const}} \tau\, \Psi_s(\tau)\, \mathrm{d}\tau + \int_{\text{const}}^\infty \frac{\tau\, \mathrm{d}\tau}{\tau^{\beta+1}} = \begin{cases} \text{const}, & \beta > 1 \\ \ln_{t\to\infty} t, & \beta = 1 \\ \infty, & \beta < 1 \end{cases} \tag{69}$$

In the case $\beta \leq 1$ the average survival time t_s is infinite. To avoid a seeming discrepancy one should understand the difference between individual events themselves and the frequencies of their occurrence (*i.e.* the probabilities). Although a particle always returns to the initial area within a finite period of time (Poincaré

theorem), the frequencies of recurrence times can be such that an average recurrence time t_{rec} will be infinite ($t_{rec} > t_s = \infty$).

We have also to recall that according to Shlesinger *et al.*[80] the real orbits of dynamical systems are always theoretically predictable because they represent solutions of a simple system of equations (for example Newton's equations). Under conditions for dynamical chaos, however, these orbits are highly unstable. Generally for chaotic motion the distance between two initially close orbits grows exponentially with time as

$$d(t) = d(0) \exp(\lambda t) \tag{70}$$

where the rate λ is called the Lyapunov exponent. This dependence holds for sufficiently long times. Local instabilities, described by eqn. (70), lead to rapid mixing of orbits within the time interval $\tau_\lambda = 1/\lambda$. Nevertheless, some properties of the system remain fairly stable and their evolution occurs at a significantly longer time-scale, $\tau_D \gg \tau_\lambda$, as a result of averaging (possibly only partially) over the fast process of mixing, caused by the instability in eqn. (70). Kinetic equations arise as a consequence of such averaging. For a discussion of the hierarchical structures in phase space and fractional kinetics see Zaslavsky and Edelman[82] and Iomin and Zaslavsky.[83] Chaotic dynamics and superdiffusion in a Hamiltonian system with many degrees of freedom was discussed by Latora *et al.*[84]

3 Approximation of classical kinetics

In the above model of reaction kinetics in renewing environments, to get the limit of classical kinetics, *i.e.* the constant specific reaction rate, one has to use the long-time approximation, $t \gg \tau_\beta$, of the Kohlrausch relaxation function (21), *cf.* Majumdar[85] and Mohanty,[86] with $\beta = 1$. This yields, *cf.* eqn. (23), $\hat{\alpha} = 1$, and then from eqn. (26)

$$k = \zeta_1^{-1} \tag{71}$$

with

$$\zeta_1 = \zeta_\alpha (\tau_\beta / \zeta_\alpha)^{1-\alpha} \tag{72}$$

This constant specific reaction rate remains renormalized by the factor leading, see below, to such phenomena as viscosity dependence of the rate constant and the compensation law. To get rid of this factor one has to reconsider the implicit assumption of a random walk modeling of reaction kinetics for very reactive intermediates. The implicit assumption is this: we are modeling reactions with high local reaction probability, P, when two reactants collide. Only for $P \rightarrow 1$ is eqn. (72) valid. The lower the numerical value of P, the closer to 1 is the apparent numerical value of α seen in computer simulations performed by Shi and Kopelman[87] for bimolecular reactions in one dimension, on a two-dimensional square lattice, on a two-dimensional critical percolation cluster, and in three-dimensional cubic lattices with various local reaction probabilities. This is the way to get $k = 1/\zeta_\alpha$ from eqns. (71) and (72), which covers the result of usual theories.

In short time-scales, well below τ_β, one finds the classical kinetics in the coupling model (CM) of Ngai[88] who restated the fundamental results of his model. In the model,

there exists a temperature-insensitive cross-over time, t_c, before which ($t < t_c$) the basic units relax independently with correlation function

$$\Phi(t) = \exp\left(-\frac{t}{\tau_0}\right) \tag{73}$$

characterized by the independent (primitive or non-cooperative) relaxation time, τ_0, and afterwards ($t > t_c$) with a slowed down non-exponential correlation function. A particularly convenient function, which is compatible with both computer simulations and experimental data, is the Kohlrausch function written in the form

$$\Phi(t) = \exp\left[-\left(\frac{t}{\tau}\right)^{1-n}\right] \tag{74}$$

where n is the coupling parameter whose value lies within the range $0 \leq n < 1$ and depends on the intermolecular interaction. What distinguishes the CM from other models that may also have simple exponential decay at short times and later a slowed down decay, is that in the other models the cross-over time t_c is strongly dependent on temperature. Realistically the cross-over occurs over a small neighborhood about t_c, where the actual relaxation function $\Phi(t)$ changes over smoothly from the exponential function to the Kolrausch function, preserving continuity of the function and its derivatives. When the width of the neighborhood is small as suggested by results of simple models, the approximate continuity of the two pieces of the correlation function at $t = t_c$ leads to the important relation

$$\tau = (t_c^{-n}\tau_0)^{1/(1-n)} \tag{75}$$

which links the effective (*i.e.* after cooperative dynamical constraints between the relaxing molecular units have been taken into account) relaxation time, τ, to the primitive (*i.e.* without taking into account the cooperative dynamical constraints) relaxation time, τ_0.

The coupling model has been applied to a wide range of physical phenomena since its inception; and it has been derived by several alternative approaches. According to Macdonald[89] over the years there have probably been well over a thousand pages, published in scientific journals and in the reports of conferences and meetings, that have been devoted to explicating and applying the model. Among the recent applications one finds *e.g.* the discussion of the breakdown of the Debye–Stokes–Einstein and Stokes–Einstein relations in glass-forming liquids,[90] explanation of the difference between translational diffusion and rotational diffusion in supercooled liquids,[91] discussion of the effects of confinement on relaxation in glass formers[92] and short-time and long-time relaxation dynamics of glass-forming substances.[93]

Most of the great body of work on the CM has directly involved Ngai and his various coauthors, and only a relatively small amount of independent discussion of the approach has appeared in the literature. Hence the importance of the critical review presented by Macdonald.[89] According to him the detailed examination and generalization of the coupling model suggested the consideration of a related, yet different, approach, the cutoff model (COM). Although both the CM and COM models involve a shorter nonzero response time, t_c, and lead to single-relaxation-time Debye response at limiting short times and high frequencies, they involve different physical interpretations of their low- and high-frequency response functions. The CM model

leads to an appreciable slope discontinuity at the t_c transition point between its two separate response parts, while the COM model shows no such discontinuity because it involves only a single response equation with a smooth transition at t_c to limiting single-relaxation-time response. See also Ngai.[94]

Viscosity dependence of specific reaction rate

Eqns. (71) and (72) enable us, *cf.* the previous report,[7] to enter the discussion on viscosity dependence of rate constants in fluids. It seems enough to recognize τ_β in relation (72) as the relaxation time of the conformational fluctuation of the reactant system. Then, if these fluctuations are driven and/or damped solely by thermal motions of solvent molecules through friction, τ_β should simply be proportional to viscosity η. Hence, from eqns. (71) and (72) one gets

$$k \sim \tau_\beta^{\alpha-1} \sim \eta^{\alpha-1} \qquad \text{for} \quad 0 < \alpha < 1$$
$$k \sim \eta^{-a} \qquad \text{for} \quad a = 1-\alpha \tag{76}$$

i.e. the form desired to fit the experimental data for the rate constant dependence on solvent viscosity, *cf.* Asano and Sumi.[95] See also Ansari[96] for viscosity dependence of the rate of conformational change in myoglobin.

As in dielectric relaxation, the distribution of the reaction rate constants may be a manifestation of one or both of the following two occurrences:[97] (i) The process occurs at different rates in different regions of the material, as would be the case if the structure was heterogeneous at a molecular level with the bulk homogenization time being longer than the measurement period. (ii) The rate constant of the process itself changes with time. In the addition polymerization process, which was of concern, new and more sterically hindered reacting sites are produced, and two types of dynamics control the polymerization rate. First is the diffusivity of the reacting groups or molecules and second is the fluctuation of the surroundings of the reacting groups, which is required to expose the reacting groups and allow them to react. Both constitute the structural relaxation process, whose rate is inversely proportional to η. In most cases η is equivalent to the average dielectric relaxation time, $\langle\tau\rangle$.

It is recalled[97] that when the reaction kinetics is mass-controlled, an increase in η at a constant T has no effect on the chemical reaction rate, but when it is diffusion-controlled an increase in η decreases the reaction rate. The situation is less straightforward when T is also changed, because the effect of T on η depends upon the magnitude of η itself. For example, when η of a liquid is low, a small change in T has a negligible effect on η. But when η is already high, the same small change in T has a very large effect on η, as is implicit in the Vogel–Fulcher–Tammann equation for viscous flow. Therefore, when the reaction is mass-controlled, cooling would decrease the rate constant mainly because the thermal energy decreases and not because η increases, and when the reaction is diffusion-controlled, cooling would decrease the average rate constant mainly because η increases, and not because the thermal energy decreases.

McAnanama *et al.*[97] have reported on the temperature-independent onset of diffusion control during polymerization in a diepoxide–amine mixture followed by

dielectric measurements. The kinetics of addition reactions in a polymerizing liquid changes from mass-controlled to diffusion-controlled when the liquid's viscosity, η, is high or the temperature, T, is low. This change occurs when the probability of reaction, initially controlled by the population of the reacting species, becomes controlled by the diffusivity of the reacting species. Diffusion-controlled kinetics may be manifested as a time-dependent reaction rate constant, which is equivalent to slow temporal decays. This is an important and a well-recognized advance in chemical reaction kinetics that has led to a discussion in terms of a distribution of the reaction rate constant instead of the usual single rate constant. It is recalled that a dispersion of the reaction rates is observed only when the reactivity of the material itself changes with reaction time, as occurs at low temperatures. However, when T is high, the reactivity does not change with time or else changes insignificantly. Its average leads to a single, time-dependent reaction rate constant. This is analogous to the dielectric relaxation phenomenon, where the distribution of relaxation rate is also broad when T is low or η is high, and it is narrow and indistinguishable from a single Debye type relaxation when T is high or η is low.

Compensation law

The compensation law or isokinetic relationship emerged after years of attempts to correlate structure and reactivity for series of reactions. In terms of the Arrhenius equation, the compensation law consists in a linear relationship between the logarithm of the pre-exponential factor and the apparent activation energy; in terms of the Eyring equation, it consists in a linear relationship between the activation entropy and the activation enthalpy. For some early examples see *e.g.* Exner,[98] and for more recent ones see Vyazovkin and Wight.[99]

The variable factor in reaction series usually is a substituent change, although solvent variation, variations of catalyst, ionic strength or pressure, and in some cases temperature, can become the variable parameter if the kinetics has been followed over a broad temperature range and the activation parameters are treated as variables.[98,99]

In classical kinetics, there is no apparent reason for the compensation law to hold. As we have shown above, in dispersive kinetics, the constant specific reaction rate, or rate constant, appears as an approximation valid to only a part of the kinetics: for reactions at time-scales much longer than those of internal rearrangements in the reaction system renewing (mixing) the environment of reactants. Even under these conditions for species reacting with high local reaction probability (when two reactants collide), the constant specific reaction rate is renormalized by a factor containing the effective time of renewing (mixing) the reactant environment, *cf.* eqn. (72). Because of this the compensation law holds, under classical approximation, for reaction series with a variable factor such as substituent change, variation of solvent, catalyst, ionic strength or pressure.

In what follows, the simple Arrhenius picture is used. Eqn. (72) is rewritten as

$$\hat{\zeta}_1 = \zeta_\alpha^\alpha \tau_\beta^{1-\alpha} \tag{77}$$

and we take

$$\zeta_\alpha = \zeta_{\alpha,0} \exp(E_{\zeta_\alpha} / RT) \tag{78}$$

and

$$\tau_\beta = \tau_{\beta,0} \exp(E_{\tau_\beta} / RT) \tag{79}$$

We have to remember, however, that the use of the Arrhenius equation for modeling relaxation in a wide temperature range is justified only for strong glass formers, see above, and therefore for fragile glass formers the parameters $\tau_{\beta,0}$ and E_{τ_β} may have no direct physical meaning. For alternative use of the Williams–Landel–Ferry equation, or Vogel–Tammann–Fulcher equations, for $T_g/T < 1$, see Angell.[39]

For $\hat{\zeta}_1$ given by eqn. (77) one can write the Arrhenius equation in the form

$$\hat{\zeta}_1 = \hat{\zeta}_{1,0} \exp(E_{\hat{\zeta}_1} / RT) \tag{80}$$

where

$$\hat{\zeta}_{1,0} = \hat{\zeta}^{\alpha}_{\alpha,0} \tau^{1-\alpha}_{\beta,0} \tag{81}$$

and

$$E_{\hat{\zeta}_1} = \alpha E_{\zeta_\alpha} + (1-\alpha) E_{\tau_\beta} \tag{82}$$

In general, for reactive species, $E_{\tau_\beta} > E_{\tau_\alpha}$ and $\zeta_{\alpha,0} > \tau_{\beta,0}$. The relations (78) and (79) intersect at the point

$$T_c = \frac{E_{\tau_\beta} - E_{\zeta_\alpha}}{R(\ln \zeta_{\alpha,0} - \ln \tau_{\beta,0})} \tag{83}$$

$$\begin{aligned} \zeta_c &= \tau_{\beta,0} \exp(E_{\tau_\beta} / RT_c) \\ &= \zeta_{\alpha,0} \exp(E_{\zeta_\alpha} / RT_c) \end{aligned} \tag{84}$$

It is easy to check that one can rewrite eqn. (80) as

$$\hat{\zeta}_1 = \zeta_c \exp\left[\frac{E_{\hat{\zeta}_1}}{R}\left(\frac{1}{T} - \frac{1}{T_c}\right)\right] \tag{85}$$

or equivalently as

$$\hat{\zeta}_1 = \hat{\zeta}_{1,0} \exp\left[\frac{T_c}{T} \ln\left(\frac{\zeta_c}{\zeta_{\alpha,0}}\right)\right] \tag{86}$$

to have the most popular forms used to present the compensation law. Also

$$\ln \hat{\zeta}_{1,0} = \ln \zeta_c - \frac{E_{\hat{\zeta}_1}}{RT_c} \tag{87}$$

which gives the desired linear relationship between the logarithm of the pre-exponential factor and the activation energy in relation (80), and

$$\hat{\zeta}_1 = \zeta_c \exp(-E_{\hat{\zeta}_1} / RT_c) \exp(E_{\hat{\zeta}_1} / RT) \tag{88}$$

In general, however, the specific reaction rate in condensed media depends on time, *cf.* Plonka.[100] The compensation law still holds. The numerical value of the dispersion parameter $\hat{\alpha}$ depends on temperature. This is the case for compensation analysis firmly entrenched in the literature on thermally stimulated techniques.

Typically, when the compensation law is reported for kinetic studies in a broad temperature range it is because of the increase of activation energy near a glass transition or some other cooperative transition. In the glass transition region, taken as a representative example, the slowing down of relaxation processes with temperature decrease occurs. Therefore, well below the glass transition one may expect to be close to the limit $\hat{\alpha} = \alpha$, and on increasing the temperature towards glass transition one may expect to approach the limit of classical kinetics $\hat{\alpha} = 1$. Accordingly, *cf.* eqn. (24), the activation energy $E_{\hat{\zeta}_\alpha}$ should approach at low temperature the limit

$$E_{\hat{\zeta}_{\hat{\alpha}}} \sim E_{\zeta_\alpha} \tag{89}$$

and at high temperature the limit

$$E_{\hat{\zeta}_{\hat{\alpha}}} = \alpha\, E_{\zeta_\alpha} + (1-\alpha)\, E_{\tau_\beta} \tag{90}$$

This phenomenon is modeled by the temperature dependence of β in eqn. (23). In the temperature range of the glass transition, *cf.* Phillips,[101] the numerical value of β changes linearly with temperature from some constant value β_g to 1.

For illustrative purposes Fig. 4 presents the Arrhenius plots of

$$\hat{\zeta}_{\hat{\alpha}} = \min(\hat{\zeta}_{\hat{\alpha}}, \zeta_\alpha) \tag{91}$$

for $\hat{\alpha} = 0.3$ and 0.7 *vs.* T_c/T. The numerical value of β changes from 0.3 to 1 in the glass transition region 1.1–1.3 in units of T/T_c, *cf.* inset in Fig. 4. Linear extrapolation of the logarithm of $\hat{\zeta}_{\hat{\alpha}}$ (dashed lines) shows the artificial compensation point at a temperature higher than T_c.

On the apparent compensation effect observed for two consecutive reactions see Budrugeac and Segal[102] and Budrugeac.[103] For parallel reaction model in decomposition kinetics see Burnham and Braun.[104]

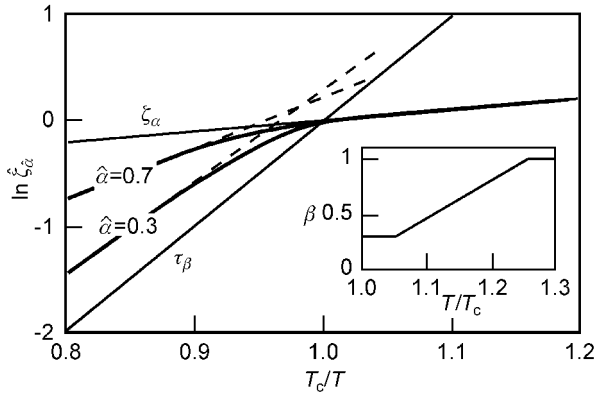

Fig. 4 Illustration of the compensation law for the activation parameters in the region of the glass transition. The dashed line intersection indicates the artificial compensation point. Details in text.

4 Kinetics in condensed media

For time-dependent specific reaction rate the potential energy barrier has to evolve in time. Taking the most familiar Arrhenius picture to relate $\hat{\zeta}_{\hat{\alpha}}$ from eqn. (26) to the activation energy $E_{\hat{\zeta}_{\hat{\alpha}}}$ by

$$\hat{\zeta}_{\hat{\alpha}} = \hat{\zeta}_{\hat{\alpha},0} \exp(E_{\hat{\zeta}_{\hat{\alpha}}} / RT) \tag{92}$$

(where $\hat{\zeta}_{\hat{\alpha},0}$ denotes the temperature-independent pre-exponential factor, T is temperature and R is the gas constant) one finds that the form (26) of $k(t)$ implies[32] the time-dependent activation energy $E(t)$ given by

$$E(t) = E_{\hat{\zeta}_{\hat{\alpha}}} + (1-\hat{\alpha}) \ln(t/\hat{\zeta}_{\hat{\alpha}}) \tag{93}$$

in units of RT, *cf.* eqn. (38).

At a first look at relation (93) one might be worried by the limit $E(t) \to -\infty$ for $t \to 0$, but there are finite mean values $\langle \ln(t/\hat{\zeta}_{\hat{\alpha}}) \rangle$ and higher moments of the distribution of logarithms of lifetime for all schemes of elementary reactions, see Plonka and Paszkiewicz.[105] From these moments one gets the moments of activation energy distributions during the reaction course

$$\left\langle [E(t) - E_{\hat{\zeta}_{\hat{\alpha}}}]^n \right\rangle = (1-\hat{\alpha})^n \left\langle \ln^n (t/\hat{\zeta}_{\hat{\alpha}}) \right\rangle \tag{94}$$

For further discussion, two kinetic schemes are of importance: first-order (or pseudo-first-order) kinetics and second-order equal-concentration kinetics. For the first-order kinetic equation with $k(t)$ given by (26), *i.e.* for

$$c/c_0 = \exp[-(t/\hat{\zeta}_{\hat{\alpha}})^{\hat{\alpha}}] \tag{95}$$

the moments of activation energy distributions are given in Box 1. For the second-order equal-concentration kinetic equation with $k(t)$ given by (26), *i.e.* for

$$c/c_0 = [1 + (t/\hat{\zeta}_{\hat{\alpha}})]^{-1} \tag{96}$$

the moments of activation energy distributions are collected in Box 2.

In a similar way one can use the Gamov formula for *e.g.* rectangular barrier permeability

$$\kappa = \exp(-qa) \tag{97}$$

with $q = 2[2m^*(V - E)]^{1/2}$ and $a = r - R$, where m^* is the effective mass of the tunneling particle, $(V - E)$ is the total energy and a is the barrier width, to find that the form (26) implies the increase, *cf.* Plonka,[106] of the tunneling distance $a(t)$, *i.e.*

$$a(t) = a(\hat{\zeta}_{\hat{\alpha}}) + q^{-1}(1-\hat{\alpha}) \ln(t/\hat{\zeta}_{\hat{\alpha}}) \tag{98}$$

The kinetic equation (95) is identical, in mathematical form, with the Kohlrausch relaxation function (21). For $\hat{\alpha} \to \alpha$ it might be physically acceptable to represent eqn. (95) in the form of a Laplace transform

From the survival probability given by

$$c / c_0 = \exp[-(t / \hat{\zeta}_{\hat{\alpha}})^{\hat{\alpha}}]$$

one finds for the distribution of $\ln(t / \hat{\zeta}_{\hat{\alpha}})$ the mean value

$$\langle \ln(t / \hat{\zeta}_{\hat{\alpha}}) \rangle = -\gamma / \hat{\alpha}$$

and the variance

$$D^2(\ln(t / \hat{\zeta}_{\hat{\alpha}})) = \pi^2 / 6\, \hat{\alpha}^2$$

where γ denotes the Euler constant. Then from

$$\langle [E(t) - E_{\hat{\zeta}_{\hat{\alpha}}}]^n \rangle = (1 - \hat{\alpha})^n \ \langle \ln^n (t / \hat{\zeta}_{\hat{\alpha}}) \rangle$$

one gets in RT units

$$\langle E(t) - E_{\hat{\zeta}_{\hat{\alpha}}} \rangle = \gamma (1 - 1/\hat{\alpha})$$

and

$$D^2 (E(t) - E\hat{\zeta}_{\hat{\alpha}}) = (\pi^2 / 6)(1/\hat{\alpha} - 1)^2$$

Box 1 First-order kinetics. Activation energy distributions.

$$\exp[-(t/\zeta_\alpha)^\alpha] = \int_0^\infty f(k) \exp(-kt)\, \mathrm{d}k, \qquad \text{or}$$
$$= \int_0^\infty g(\zeta) \exp(-t/\hat{\zeta})\, \mathrm{d}\zeta \tag{99}$$

for $g(\zeta) = f(1/\zeta)/\zeta^2$, and to interpret eqn. (95), like the Kohlrausch relaxation function (21) in some applications, in terms of the superposition of monoexponential decays distributed continuously with density given by $f(k)$ or $g(\zeta)$.

It follows from eqn. (99) that the density of $f(k)$ can be found as an inverse Laplace transform. Although the inverse transforms are known exactly only for numerical values of α equal to 1/3, 1/2 and 2/3, there is no problem with other numerical values of α, *cf.* the previous review.[7] The problem is that $f(k)$ is the density of a stable distribution with no moments. No moments of $f(k)$ and time dependence of the rate coefficient for stretched exponential decay were always seen as some disadvantages in this kind of interpretation of experimental results fitted with a Kohlrausch relaxation function. However, for the cases when there are reasons to believe that distributions of

From the survival probability given by

$$c/c_0 = [1 + (t/\hat{\zeta}_{\hat{\alpha}})^{\hat{\alpha}}]^{-1}$$

one finds for the distribution of $\ln(t/\hat{\zeta}_{\hat{\alpha}})$ the mean value

$$\langle \ln(t/\hat{\zeta}_{\hat{\alpha}}) \rangle = 0$$

and the variance

$$D^2(\ln(t/\hat{\zeta}_{\hat{\alpha}})) = \pi^2/3\,\hat{\alpha}^2$$

Then, from

$$\langle [E(t) - E_{\hat{\zeta}_{\hat{\alpha}}}]^n \rangle = (1-\hat{\alpha})^n \ \langle \ln^n(t/\hat{\zeta}_{\hat{\alpha}}) \rangle$$

one gets in *RT* units

$$\langle E(t) - E_{\hat{\zeta}_{\hat{\alpha}}} \rangle = 0$$

and

$$D^2(E(t) - E_{\hat{\zeta}_{\hat{\alpha}}}) = (\pi^2/3)(1/\hat{\alpha} - 1)^2$$

Box 2 Second-order equal-concentration kinetics. Activation energy distributions.

lifetime displayed by a Kohlrausch relaxation function originate from a prior distribution of monoexponential decays, it is worth noting that there are moments of $g(\zeta)$ for $\zeta = 1/k$. Furthermore, these moments are directly related to those of $g(t)$ following from eqn. (95),

$$\langle t^n \rangle = n! \langle \zeta^n \rangle \tag{100}$$

The moments of $g(t)$, easy to calculate directly from eqn. (95), are given by

$$\langle (t/\hat{\zeta}_{\hat{\alpha}}) \rangle = \Gamma(1 + n/\alpha) \tag{101}$$

where Γ denotes the Gamma function. Because of eqns. (100) and (101) one has

$$\langle (\zeta/\zeta_\alpha)^n \rangle = (1/n!)\Gamma(1 + n/\alpha) \tag{102}$$

cf. Weron[107] and Lindsey and Patterson.[108]

Even more remarkable is the existence of moments for $g(\ln \zeta)$ and their simple relationships to those of $g(\ln t)$,

$$\langle \ln t \rangle = \langle \ln \zeta \rangle - \gamma \tag{103}$$

and

$$D^2(\ln t) = D^2(\ln \zeta) + \pi^2/6 \tag{104}$$

Making use of these findings, the results collected in Box 3 were obtained.[105]

In analogy to eqn. (99) one can write for the second-order equal-concentration kinetic eqn. (96)

$$\frac{1}{1+(t/\zeta_\alpha)^\alpha} = \int_0^\infty \frac{g(\zeta)}{1+t/\zeta}\,\mathrm{d}\zeta \tag{105}$$

which leads[105] to the results collected in Box 4.

See also Edholm and Blomberg[109] for a discussion of stretched exponentials and barrier distributions, and Skulski[110,111] for the method of estimating the width of a Gaussian-logarithmic distribution of relaxation times in relaxor materials.

Reaction course in fluids

We have to recall the statement of Edelstein and Agmon[112] that much of current study of chemical kinetics, from gas-phase dynamics to surface reactions, centers on understanding the factors governing rate coefficients. While such studies are of

From the integral transform

$$\exp[-(t/\xi_\alpha)^\alpha] = \int_0^\infty f(\tau)\exp(-t/\tau)\,\mathrm{d}\tau$$

one gets

$$\langle \ln t \rangle = \langle \ln \tau \rangle - \gamma$$

and

$$D^2(\ln t) = D^2(\ln \tau) + \pi^2/6$$

which yield in *RT* units

$$\langle E(t) - E_{\zeta_\alpha} \rangle = \langle E(\tau) - E_{\zeta_\alpha} \rangle$$

and

$$D^2(E(t) - E_{\zeta_\alpha}) = D^2(E(\tau) - E_{\zeta_\alpha}) - (\pi^2/3)(1/\alpha - 1)$$

Box 3 First-order kinetics. Rigid-matrix approximation.

From the integral transform

$$\frac{1}{1+(t/\zeta_\alpha)^\alpha} = \int_0^\infty \frac{f(\tau)\,\mathrm{d}\tau}{1+t/\tau}$$

one gets

$$\langle \ln t \rangle = \langle \ln \tau \rangle$$

and

$$D^2(\ln t) = D^2(\ln \tau) + \pi^2/3$$

which yield in RT units

$$\langle E(t) - E_{\zeta_\alpha} \rangle = \langle E(\tau) - E_{\zeta_\alpha} \rangle$$

and

$$D^2(E(t) - E_{\zeta_\alpha}) = D^2(E(\tau) - E_{\zeta_\alpha}) - (2\pi^2/3)(1/\alpha - 1)$$

Box 4 Second-order equal-concentration kinetics. Rigid-matrix approximation.

fundamental interest and importance, the concomitant neglect of a more rigorous and comprehensive study of the time course of chemical reactions is unjustified. This statement finds little support as this area continues to develop rapidly.

Kim *et al.*[113] presented efficient numerical methods for solving kinetic equations for various diffusion-influenced bimolecular reactions. The finite difference method is used to solve diffusion reaction equations for the pair distribution function, and the Runge–Kutta method, with an adaptive time step, is used to evolve the kinetic equation for the concentration. These methods were applied to the classical one- and three-dimensional Smoluchowski approach for diffusion-influenced binary reactions, which can be solved exactly, and therefore the numerical accuracy can be easily compared with the analytical solutions. The reported results[114] show remarkable accuracy and speed. Exact solution of the reversible diffusion-influenced reaction for an isolated pair in three dimensions was given by Kim and Shin.[115] See also Nassif and Silva,[116] Agmon and Gopich[117] and Solc.[118]

Barzykin *et al.*[119] have addressed the problem of diffusion-assisted reactions on micelle surfaces. An exact matrix form solution for the pair survival probability satisfying the diffusion equation with a distance-dependent reaction term has been presented and analyzed together with several useful approximations. Matrix solution is computationally superior to numerical integration of the partial differential

equation. For its use for the case of photoinduced electron transfer followed by back-transfer see Barzykin *et al.*[120] Solvation dynamics in micelles was discussed by Pal *et al.*[121]

For irreversible fluorescence quenching in solution, it is shown by Naumann[122] that the kinetic prediction of the Smoluchowski approach, which is exact under target model conditions, can also be alternatively formulated in terms of well-defined non-Markovian rate equations. For the superposition approximation, it was demonstrated that the definition of an approximate quenching constant can also be formally transferred to the reversible quenching process if only the low-density limits of the net forward rate kernels in the generalized rate equations are known. Fluorescence quenching by reversible excimer formation and by reversible excitation transfer meets this requirement.

In one dimension, Redner and Krapivsky[123] have studied the capture of a diffusing 'lamb' by diffusing 'lions'. The capture dynamics is exactly soluble by probabilistic techniques when the number of lions is very small, and is tractable by extreme statistical considerations when the number of lions is very large. However, the exact solution for the general case of three or more lions is still not known. For the same, one-dimensional system, Kuzovkov *et al.*[124] have considered front propagation in the autocatalytic scheme $A + B \rightarrow 2A$ where A particles are allowed to decay, $A \rightarrow 0$, with a constant decay rate. Tabata and Kuroda[125] have discussed the diffusion-controlled $A + A \rightarrow 0$ reaction of non-equilibrium states on a disordered linear-chain lattice. The problem of diffusion-influenced reversible trapping in one dimension was discussed by Kim and Shin.[126]

Kipriyanov *et al.*[127] presented a new approach to the derivation of binary non-Markovian kinetic equations which was used subsequently for discussion of the irreversible reactions $A + B \rightarrow C$ and $A + B \rightarrow C + D$ in spatially non-uniform systems[128] and of the effect of chemical displacement of B species,[129] due to chemical conversion events, on kinetics of reaction $A + B \rightarrow B$.

Sung and Lee[130] introduced the non-equilibrium function formalism for diffusion-influenced bimolecular reactions. This formalism was used for the kinetics of reversible energy transfer reactions[131] and relations among the modern theories of diffusion-influenced reactions were discussed.[132,133]

Benichou *et al.*[134] have studied the kinetics of diffusion-limited, pseudo-first-order $A + B \rightarrow B$ reactions in the situation in which the particles' intrinsic reactivities are not constant but vary randomly in time. The particles are supposed to bear 'gates' which fluctuate in time, randomly and independently of each other, between two states—an active state, when the reaction may take place between A and B particles appearing in close contact, and a blocked state, when the reaction is completely inhibited. For the theoretical analysis of the influence of stochastic gating on the transient effect in fluorescence quenching by electron transfer see Bandyopadhyay *et al.*[135]

Graber[136] introduced a reaction diffusion model on a lattice involving two particles species, A and B. B particles initially fill the lattice, and A particles diffuse, transforming B particles to A particles each time they meet. He keeps the number of A particles constant, eliminating the oldest ones. The process builds empty clusters whose short-time features are fractal (in the universality class of invasion percolation) and whose long-time features are those of compact objects.

Syutkin[137] studied the A + B → A reaction by computer simulation of random walks of particles A on a simple cubic lattice with *randomly* removed bonds above the percolation threshold. The B particles are immobile. It is shown that at low concentration of walkers, the non-exponential decay of B particles originates mainly from the rate constant distribution. At small times, the anomalous diffusion of walkers contributes to the non-exponential kinetic behavior as well. The distribution of specific reaction rates arises due to different configurations of removed bonds around the B particles.

Model chemical reactions are very specific objects of study, since despite their simply structured 'rules of the game' they display very rich temporal patterns of behavior.[138] From the point of view of simulations, model chemical reactions present the important advantage that in several particular cases exact solutions (or at least, asymptotic behaviors) are known; this provides then an excellent test for the numerically obtained results. On the other hand, analytical approximations may be quite misleading, when pushed beyond their (often poorly known) limits of validity. In several, very important instances, computer simulations have played a decisive role in showing that well-established patterns of thought were incorrect. In many cases the plotted results of simulations are intuitively easy to grasp; this has helped very much in establishing new ways of understanding the underlying phenomena. As an example, Nechaev *et al.*[139] have studied the dynamics of an isolated Rouse chain, which diffuses in a three-dimensional space under the constraint that one of its extremities, the slip-link, may move only along a line containing randomly placed immobile traps. For such a model they have computed exactly the time evolution of the probability $P_{sl}(t)$ that the slip-link will not encounter any of the traps until time *t*, *i.e.* that the chain will remain completely mobile until this moment of time. They have shown that in the most general case this probability is a succession of several stretched-exponential functions of time, where the dynamical exponents depend on the time of observation and on characteristic cross-over times. They have specified these cross-over times and have determined explicitly the forms of $P_{sl}(t)$ in several particular situations. They expect their results to serve as benchmarks in more complex situations, which are not amenable to a fully analytical treatment. Thus programs involving realistic computer simulations can be tested by comparing the results to their exact expressions. See also Ilan and Loring.[140]

Kim and Shin[141] have investigated the single-species diffusion-influenced reaction A + A → *a*A with a finite reactivity, in all dimensions. The reaction model includes a pure coagulation ($a = 1$) or a pure annihilation ($a = 0$) model. They have applied the hierarchical Smoluchowski approach to study the dimensional aspects of the fluctuations, reactivity, particle size and a ($0 \leq a \leq 1$). The theoretical results were compared with those of Monte Carlo simulations in one, two and three regular dimensions. The simulation results revealed that the classical Smoluchowski approach is exact in the short-time limit in all dimensions and in the long-time limit in three dimensions. The hierarchical Smoluchowski approach was found to be numerically exact at all times in two and three dimensions. For one dimension, a numerical method is presented to obtain the exact results of the annihilation for a finite reactivity.

The kinetics and thermodynamics of folding a representative sequence of a 125-residue protein model subject to Monte Carlo dynamics on a simple cubic lattice were investigated by Dinner and Karplus.[142] The 125-mer folding reaction is

particularly attractive in that it exhibits complexities comparable to those observed for real proteins but it is still simple enough that its kinetics and thermodynamics can be explored fully. Du *et al.*[143] have considered a 48-mer lattice model in their study of the effects of geometrical restrictions, including those of chain connectivity and steric excluded volume, on protein folding. For the estimation of the minimum length of a protein chain required for expeditious and robust folding into a specific target motif see Fernández *et al.*[144]

Brownian dynamics simulations were used by Kim *et al.*[145] to study the long-time behavior of a reversible diffusion-influenced reaction perturbed by photolysis, and by Yang *et al.*[146] for calculation of the time-dependent rate coefficients of diffusion-influenced reactions.

Fast events in protein folding were recently reviewed by Callender *et al.*[147] and Gruebele.[148] Understanding how proteins fold up into their compact three-dimensional forms is a central problem in modern structural biology.[147] The reason is that the particular structure of a protein governs its specific activity, and any biological function is supported by a corresponding protein system. It is recognized that the spatial structure of a protein molecule is determined completely by the sequence of amino acids of its polypeptide chain, at least for small proteins and probably for all proteins in a general sense. Moreover, the amino acid sequence also codes the way the three-dimensional structure is reached efficiently, *cf.* Wang and Wang.[149,150] Both aspects are equally important for protein engineering purposes, because any polypeptide sequence coding a new protein must not only offer some new function but also ensure its efficient folding. Otherwise, the expressed protein might never accumulate in large quantities because slow folding processes may permit the accumulation of long-lived metastable non-functional folds. Besides, aggregation at intermediate stages or digestion by the proteinases of the host will be high for long-lived unfolded structures. The folding of a protein is a process both expeditious and robust, *cf.* Fernández and Berry.[151] Their analysis of this process uses a coarse discretized representation of the evolving form of the backbone chain, based on its torsional states. The properties expeditious and robust, imply that the folding protein must have some tolerance to both torsional 'frustrated' and side-chain contact mismatches which may occur during the folding process. See also Fernández *et al.*[152] The role of the energy gap, between misfolded states and native state, in folding dynamics is discussed by Pitard and Orland.[153] It is stressed[147] that for several decades there has been much effort toward determining the kinetics of how a protein folds from its extended unfolded conformation to its final compact form. Investigators have sought to answer the questions of what types of structures form first and on what time-scales. Of most importance are the early kinetics events. These events set up all that are to follow in the guided pathway. However, the early kinetics of the folding pathway occur generally on the submillisecond time-scale, and this has been a difficult time-scale to access experimentally since the typical approach, stopped-flow devices whereby two reactants are mixed and the chemical reaction launched, have been limited to a resolution of 1–10 ms, and only recently has a rapid solution mixer with a 100 μs deadtime been developed.[154]

For new approaches that are capable of initiating and monitoring the fast events in protein folding with temporal resolution down to picoseconds see the above-mentioned reviews[147,148] and also Eaton *et al.*[155]

Highly non-exponential folding kinetics in aqueous solution have been observed by Sabelko *et al.*[156] during temperature jump induced refolding of two proteins, yeast phosphoglycerate kinase and a ubiquitin mutant. For phenylacetylene oligomer, which is known to acquire a solvophobically driven helical structure at low temperatures, Yang *et al.*[157] have reported the transition from exponential to non-exponential kinetics during helix formation at low temperatures. See also Parak and Achterhold[158] and Prusakov *et al.*[159]

Volk *et al.*[160] explored the early folding process involving local collapse and helix formation of *de-novo* peptides with a disulfide bond between two modified tyrosines (Y′) linking the ends of a 17-amino-acid polypeptide chain Y′$(AAAAK)_3$Y′ (with A ≡ alanine and K ≡ lysine), constraining it to a non-native, more randomly coiled conformation. The ultrafast (subpicosecond) process triggering the folding constitutes the photodissociation of the disulfide S–S bond. These experiments provide information on the kinetics of α-helix formation, which is interrogated by the recombination dynamics of the thiyl radical pair at the time-scale from 1 ps to 10 μs. A significant novel result emerging from the studies of Volk *et al.*[160] is the failure of conventional kinetic schemes to describe this process. Over a time range of seven orders of magnitude the radical concentration exhibits an extremely non-exponential time dependence.

Volk *et al.*[160] analyzed their data using the stretched exponential, eqn. (95). The validity of this analysis was confirmed by Metzler *et al.*[161] and the reported numerical values of the parameters of eqn. (95) are $\hat{\zeta}_{\hat{\alpha}} = 1.5 \pm 1.2$ fs for $\alpha = 0.086 \pm 0.03$. Furthermore, the same set of experimental data was subjected to alternative analysis in terms of a power law, eqn. (96). An equally good fit as with the use of eqn. (95) is reported for eqn. (96) with $\hat{\zeta}_{\hat{\alpha}} = 7 \pm 1$ ps and $\alpha = 0.331 \pm 0.04$.

Scanning the experimental data, fig. 1 in the paper of Metzler *et al.*,[161] we have confirmed the above results, finding the numerical values of the difference absorbance corresponding to $c(0)$ in eqn. (95) for $\hat{\zeta}_{\hat{\alpha}} = 1.53$ fs and $\hat{\alpha} = 0.086$ to be equal to 0.0586, and of the difference absorbance corresponding to $c(0)$ in eqn. (96) for $\hat{\zeta}_{\hat{\alpha}} =$ 7 ps and $\alpha = 0.331$ to be equal to 0.0156. For these numerical values of parameters, *cf.* upper part of Fig. 5, there is no marked difference between stretched exponential (solid line) and power law (dashed line) in the range covered by the experimental data. The reported fits, *cf.* insets, seem to be really equally good. A marked difference is seen, however, when the fitting equations are used to calculate the distribution functions for the logarithms of lifetimes in the form $F = 1 - (A/A_0)$ *vs.* log t or their densities given by $f = \mathrm{d}F/\mathrm{d} \ln t$. According to the fit with the stretched exponential, less than 20% of the transient absorption of the thiyl radicals is followed. According to the power law, the value is about 70%, *cf.* middle part of Fig. 5.

The phenomenological description of the kinetics, which is characterized either by the stretched exponential [eqn. (95)] or the power law [eqn. (96)], is not sufficient to determine a particular mechanism for the folding reaction. In general, two classes of mechanisms, *i.e.* inhomogeneous or homogeneous kinetics, can yield such non-exponential long-tailed time dependence. Metzler *et al.*[161] have focussed on the inhomogeneous kinetics assuming that each peptide molecule recombines exponentially in time, with a characteristic time-independent rate, but each molecule is characterized by a different rate. In their notation the total time evolution in the inhomogeneous system is then given as a superposition of the simple individual

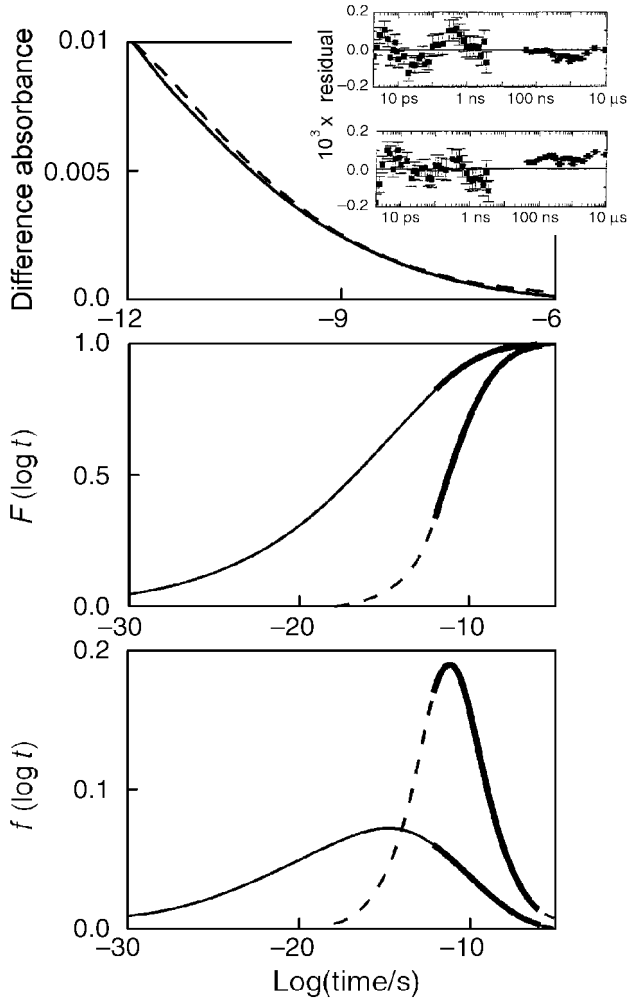

Fig. 5 Analysis of data of Volk *et al.*[160] on peptide folding. Details in text.

decays with a distribution function of the lifetimes, $f_j(\tau)$, with $j = 1$ and $j = 2$ for the stretched-exponential and the power law, respectively. The stretched exponential description, *cf.* eqns. (95) and (99), was then given in terms of the Laplace transform written as

$$\exp[(-t/\tau)^{\alpha}] = \int_0^{\infty} \mathrm{d}\tau \; f_1(\tau)\exp(-t/\tau) \tag{106}$$

and in a similar way

$$\left[1+(t/\tau'_0)^{\beta}\right]^{-1} = \int_0^{\infty} \mathrm{d}\tau \; f_2(\tau)\exp(-1/\tau) \tag{107}$$

Taking $g(t/\tau_0) = C(t)/C(0)$ one gets, *cf.* eqn. (99),

$$g(t/\tau_0) = \int_0^{\infty} \mathrm{d}\tau \; f(\tau)\exp(-1/\tau) \tag{108}$$

For $p = 1/\tau$, *i.e.* $\mathrm{d}\tau = -p^{-2}\,\mathrm{d}p$ one has

$$g\left(\frac{1}{\tau_0}\right) = \int_0^{\infty} \mathrm{d}p \; \frac{f(1/p)}{p^2}\exp(-pt) \equiv L\left\{\frac{f(1/p)}{p^2};t\right\} \tag{109}$$

i.e. $g(t/\tau_0)$ is the Laplace transform of $p^{-2}f(1/p)$, and $f(\tau)$ is given by

$$f(1/p) = p^2 L^{-1}\{g(t/\tau_0);p\} \tag{110}$$

and

$$f(\tau) = f(1/p \to \tau) \tag{111}$$

Introducing the Fox function representation, Metzler *et al.*[161] calculated the inverse transform in a closed form solution. The Fox functions are

$$g_1(t) = \exp[(-t/\tau_0)^{\alpha}] = \frac{1}{\alpha} H_{0,1}^{1,0}\left[\frac{t}{\tau_0}\middle|\left(0,\frac{1}{\alpha}\right)\right] \tag{112}$$

and

$$g_2(t) = \frac{1}{1+(t/\tau'_0)^{\beta}} = \frac{1}{\beta} H_{1,1}^{1,1}\left[\frac{t}{\tau'_0}\middle|\frac{(0,1/\beta)}{(0,1/\beta)}\right] \tag{113}$$

for the two above relaxation functions, respectively. Applying the inverse Laplace transform they get

$$f_1\left(\frac{\tau}{\tau_0}\right) = \frac{1}{\alpha\tau} H_{1,1}^{1,0}\left[\frac{\tau}{\tau_0}\middle|\frac{(0,1)}{(0,1/\alpha)}\right] \tag{114}$$

and

$$f_2\left(\frac{\tau}{\tau_0}\right) = \frac{1}{\beta\tau} H_{1,2}^{1,1}\left[\frac{\tau'_0}{\tau}\middle|\frac{(1,1/\beta)}{(1,1/\beta),(1,1)}\right] \tag{115}$$

Asymptotically, for $\tau \gg \tau_0$,

$$f_1\left(\frac{\tau}{\tau_0}\right) \sim \frac{1}{\alpha\tau_0(\tau/\tau_0)} \frac{\alpha^{(2\alpha-1)/(2-2\alpha)}}{\sqrt{2\pi(1-\alpha)}} \left(\frac{\tau}{\tau_0}\right)^{\alpha/(2-2\alpha)} \exp\left\{-(1-\alpha)\alpha^{\alpha/(1-\alpha)}\left(\frac{\tau}{\tau_0}\right)^{\alpha/(1-\alpha)}\right\} \tag{116}$$

which differs from the expression given in the previous review[2] by the prefactor, and

$$f_2\left(\frac{\tau}{\tau_0}\right) \sim \frac{1}{\tau'_0\Gamma(\beta)}\left(\frac{\tau}{\tau'_0}\right)^{-1-\beta} \tag{117}$$

A model is outlined[161] which leads to a stretched-exponential or to a power-law recombination depending on the competition between energetic and entropic trends. It is assumed that upon cleavage of the S–S bond each peptide starts recombining from a 'distance' L of an unrecombined configuration. L is defined in some space of possible configurations and the typical recombination time starting from L is $\tau(L)$. Therefore

$$\frac{C(t)}{C(0)} = \int_0^\infty \mathrm{d}L\ f(L) \exp[-t/\tau(L)] \tag{118}$$

where $f(L)$ is the distribution of distances. Following Palmer *et al.*[162] it is assumed that

$$f(L) = f_0\lambda^{-1} = f_0 \exp(-L \ln \lambda) \tag{119}$$

For

$$\tau(L) = \tau_0 \exp(aL) \tag{120}$$

one has

$$C(t) \sim t^{-\ln\lambda/a} \tag{121}$$

where the constants λ and a are independent of L and t.

For the scaling

$$\tau(L) = \tau_0 L^\eta \tag{122}$$

eqns. (118), (119) and (122) result in

$$C(t) \sim \exp[-(Kt)^{1/(1+\eta)}] \tag{123}$$

This somewhat oversimplified model might be nicely supplemented by Angell's[163] discussion of the energy landscape concepts and the folding transition in proteins, and comments of Oliveberg[164] on an alternative explanation for 'multistate' kinetics in protein folding, namely transient aggregation and changing transition-state ensembles.

Analysis of a fractal Michaelis–Menten curve has been presented by Heidel and Maloney.[165]

Fluid–solid transition

A triumph of modern theoretical physics is the notion that rigidity and orderliness go together, see Wolynes.[166] A periodic array of atoms is recognizable and globally different from a fluid. Pushing at it in one place causes no rearrangement because a local disturbance will be met by a collective response of the whole. The rigidity of glass, an amorphous solid, remains mysterious. Without any apparent order, a chaotic jumble of atoms behaves as if rigidly frozen.

According to Suga[167] our knowledge of amorphous solids is quite poor compared with that of crystalline solids. Most pure substances can be obtained, in principle, in crystalline as well as non-crystalline states by physical and chemical methods. Destruction of three-dimensional periodicity in crystalline substances produces novel properties which cannot be anticipated from knowledge of crystal sciences. One direction of materials science in the coming century will surely be a new realm of amorphous condensed matter science.

Crystallization. Kinetics in systems undergoing a first-order phase transition are important in many scientific and technological disciplines, *cf.* Ramos *et al.*[168] At the end of the 1930s Kolmogorov, Johnson and Mehl, and Avrami (KJMA) introduced a simple theory describing the decay of a metastable system towards a unique equilibrium phase. To learn when, where and what the above-mentioned four scientists have written about the model named after them, see Fanfoni and Tomellini[169] and Korobov.[170] The basic assumptions are simple: negligible small 'droplets' of the equilibrium phase nucleate from the metastable phase and subsequently grow without substantial deformation. The growing droplets are assumed to be randomly placed and overlap freely, with the result that the remaining volume fraction occupied by the metastable phase decays as

$$V(t) = \exp[-V_e(t)] \tag{124}$$

where V_e is the so-called extended volume of the transformed phase, that is the volume the transformed phase would acquire if the overlap among the growing nuclei were disregarded. Typically, *cf.* Weinberg *et al.*,[171] $V_e(t)$ is given by

$$V_e(t) = kt^n \tag{125}$$

where k is a constant and n is an integer or half-integer. Introducing eqn. (125) into eqn. (124) one gets

$$V(t) = \exp(-kt^n) \tag{126}$$

The exponent n is termed the Avrami exponent, and from eqn. (126) it can be seen that this quantity is the slope in a plot of $\ln \ln V(t)^{-1}$ *vs.* $\ln t$, termed an Avrami plot.

For the use of traditional Avrami analysis for crystallization kinetics of syndiotactic polypropylene, see Supaphol and Spruiell.[172] The same authors[173] have compared the use of Avrami analysis with three other macrokinetic models, namely those of Tobin,[174] Malkin,[175] and the so-called simultaneous Avrami model. Judging from the quality of fit only the Avrami, Malkin and simultaneous Avrami models were found to describe the time dependence of the relative crystallinity well, resulting in the rejection of the Tobin model in describing the isothermal crystallization of syndiotactic polypropylene. See also Supaphol.[176]

The original KJMA relation was derived for isothermal conditions and cannot be used to fit experimental results obtained with variable temperature, *cf.* Frade,[177] Lambrigger[178,179] and Oliveira *et al.*[180] All these authors assume the Nakamura[181–183] approach as a convenient basis for interpreting the kinetics of crystallization with constant rate of temperature change. Eqn. (126) is rewritten as

$$V(t) = \exp\left[-\left(\int_0^t k(T)\,\mathrm{d}\tau\right)^n\right] \tag{127}$$

and for a constant rate of cooling or heating, q, one gets

$$V(t) = \exp\left[-\frac{1}{q^n}\left(\int_0^T k(T)\,\mathrm{d}T\right)^n\right] \tag{128}$$

or

$$V(t) = \exp[-\chi(T)/q^n] \tag{129}$$

where

$$\chi(T) = \left[\int_0^T k(T)\,\mathrm{d}T\right]^n \tag{130}$$

is the heating or cooling function, *cf. e.g.* Chuah *et al.*[184] To get one of the most widely used solutions for experiments performed on heating at constant rate q, *i.e.*

$$\ln[-\ln V(t)] = \text{const} - n \ln q - \frac{E}{R}T^{-1} \tag{131}$$

one has to take the Arrhenius temperature dependence of k in eqn. (126) and to use the formal relation $k(T) = k^{1/n}$.

For the use of the Avrami equation for non-isothermal transformation kinetics see also Lu *et al.*,[185] Grong and Myhr,[186] Málek *et al.*[187] Martins and Cruz-Pinto[188] and Vázquez *et al.*[189]

The idealizations made in formulating the KJMA equation are under vivid discussion, see *e.g.* Carter's[190] discussion of ion-irradiation-induced amorphization processes in semiconductors, and Málek's[191,192] remarks on the autocatalytic model.

The impingement among clusters has been taken into account in the framework of Avrami's statistical approach.[193–195] At first the system has been considered in which nucleation occurs at a given number of pre-existing sites randomly distributed throughout the whole surface. The results obtained by numerical computations indicate that particular conditions can indeed be realized for which the photoelectron signal is chiefly related to the kinetics of the surface fraction that is covered by islands. A more involved system has also been modeled where nucleation does not occur at pre-existing sites but throughout the formation of stable dimers. Under this

circumstance, Avrami's treatment of island impingement can still be retained although now a system of integral differential equations has to be solved to get the kinetics. Such a modeling should be suitable for describing the metallic film growth studied by photoelectron signals. See also Fanfoni *et al.*[196] and Tomellini and Fanfoni.[197]

The time evolution of the total perimeter of clusters growing on a surface has been described by Tomellini and Fanfoni[198] on the basis of the KJMA theory. A general formula, which can be easily extended to any space dimension, was obtained. When particular nucleation functions and the cluster growth law are considered the kinetics of the perimeter can be explicitly calculated and, moreover, it can be expressed as a function of the covered surface. Experimental data on the efficiency of a Cu/CuO_x model catalyst, towards imide formation, have been satisfactorily described by the model. Moreover, the growth of Ag on a GaAs(110) surface studied *via* photoelectron spectroscopy has been qualitatively explained by the proposed model. In the model case of cylindrical clusters knowledge of the evolution of the total perimeter allows the entire area of the film to be evaluated. Microstructure development in KJMA theory and growth kinetics were discussed by Pineda and Crespo.[199]

For detailed discussion of rate equations and KJMA method for modeling the coverage–time dependence in thin-film growth at solid surfaces, see Volpe *et al.*[200]

Vitrification. The glass transition remains to be considered as 'the deepest and most interesting unsolved problem in solid-state theory', *cf.* Angell[201] and Lunkenheimer *et al.*[202] However, we may be closer to a breakthrough in the understanding of the glassy state than ever before in the long history of the glassy research.[202–204] Most recent studies focus on the dynamic behavior of glasses and their high-temperature precursors, the supercooled liquids. Spatially heterogeneous dynamics in supercooled liquids was reviewed by Ediger.[205] As the liquid is cooled below its melting point, dynamics slow dramatically, typically by more than 10 orders of magnitude before the transition to a glass occurs. A qualitative change in the character of molecular motion occurs with this slowing of dynamics. Near the glass transition, dynamics in one region of supercooled liquid can be orders of magnitude faster than dynamics in another region only a few nanometres away. This heterogeneity in dynamics has important consequences for understanding transport properties and the kinetics of chemical reactions in such materials.[205]

Dynamic heterogeneity is an active field of glass transition research. The length scale of this heterogeneity is called the characteristic length. It can be calculated from complex heat capacity curves in the equilibrium liquid or from dynamic calorimetry curves corrected with regard to non-equilibrium. No molecular parameters or microscopic models are necessary to obtain the length. Hempel *et al.*[206] have reported the characteristic length near the glass transition temperature for about 30 glass formers including small-molecule liquids, polymers, silica glasses, a metallic glass, a liquid crystal and a plastic crystal. The lengths are between 1.0 and 3.5 nm. See also Donth *et al.*[207] and Wang and Ediger.[208] Russina *et al.*[209] have presented experimental evidence for fast heterogeneous collective structural relaxation in supercooled $Ca_{0.4}K_{0.6}(NO_3)_{1.4}$ near the glass transition temperature. Wang and Ediger[210] have determined the lifetime of spatially heterogeneous dynamic domains in polystyrene melts.

It has long been debated[2] whether the dynamical complexity described by the stretched exponential is intrinsic, with all regions of the sample exhibiting a similar non-exponential response, or whether it is the result of heterogeneity, with localized degrees of freedom relaxing exponentially but with a distribution of relaxation time. Several studies, *cf.* Schiener *et al.*,[211] of supercooled liquids near their calorimetic glass transition temperature have concluded that heterogeneity occurs on length scales of 1 to 5 nm. These domains are not static but their distinct relaxation rates persist long enough to cause the broadened response. Schiener *et al.*[211] have shown that large-amplitude, low-frequency electric fields can be used to burn spectral holes in the dielectric response of supercooled propylene carbonate and glycerol. This ability to selectively modify the dielectric response establishes that the non-Debye behavior results from a distribution of relaxation times. Refilling of the spectral hole was consistent with a single recovery time that coincided with the peak in the distribution. Moreover, refilling occurred without significant broadening, which indicates negligible direct exchange between the degrees of freedom that responded to the field. Non-resonant spectral hole burning facilitates direct investigation of the intrinsic response of systems that exhibit non-exponential relaxation.

Different kinds of static and dynamic heterogeneity at the glass transition, in relation to recent experiments, were discussed by Sillescu.[212] He states that during the last few years a number of experimental methods have been developed whereby a dynamically distinguishable sub-ensemble can be selected in a supercooled liquid close to T_g and its return to the full equilibrium ensemble can be subsequently monitored. These experiments provide a pragmatic way of quantifying heterogeneity *via* the selection procedure. For example, one can decompose a relaxation function $\Phi(t)$, approximated by a stretched exponential with β_{hom}, into a superposition of *intrinsic* stretched exponentials with β_K. The 'degree of heterogeneity'

$$\eta = (\beta_{\text{hom}} - \beta_K)/(1 - \beta_K) \tag{132}$$

with $0 < \beta_K \leq 1$, $\beta_K \leq \beta_{\text{hom}} \leq 1$ and $0 < \eta \leq 1$, vanishes in the homogeneous limit and is unity in the heterogeneous limit. Of course, η may depend upon how sub-ensembles are filtered out in a particular selection experiment; however, it is of value for comparing different systems studied by the same experimental procedure. It should be noted that η has also been determined in studies of time-resolved solvation spectroscopy where no selection procedure is involved.

During recent years, the mode-coupling theory has been developed as a model for the dynamics of strongly interacting disordered matter. The mode-coupling theory for the density fluctuation dynamics of simple liquids was developed originally in order to deal with the cage effect, see Götze.[213] This effect has been known for some time as the essential feature distinguishing the dynamics of a liquid from that of a dense gas. It is worth noting that the transition from the dynamics of isolated molecules to that of a bulk liquid was observed for the first time by analyzing the dielectric relaxation (10^{-2}–10^{9} Hz) of ethylene glycol (EG) guest molecules confined to zeolitic host systems of different topology. Beyond a threshold channel size the liquid character is lost, indicated by a dramatically increased relaxation rate and an Arrhenius-like temperature dependence. Computer simulations of the molecular arrangement in a confining space prove that an ensemble as small as six molecules is sufficient to exhibit the dynamics of a bulk liquid, see Huwe *et al.*[214] and Kremer *et al.*[215]

Molecular dynamics of glass-forming liquids speeds up dramatically, resulting in a decrease in glass transition temperature, when the material is confined in pores of nanometre scale, *cf.* Ngai.[92,216] For dynamics of confined water see also Bellissent-Funel.[217]

Returning to the mode-coupling theory,[213] it was discovered that the derived equations of motion, which deal with a self-consistent treatment of density-fluctuation propagating and current relaxations, lead to a bifurcation of the long-time limit of the density correlators. This bifurcation provided a model for an ideal liquid-to-glass transition. The identification of this glass transition singularity opened up the possibility for an analytic solution of the complicated nonlinear equations by means of asymptotic expansions using the distance from the transition point as a small parameter. It turned out that the bifurcation is connected with a novel dynamical scenario. A set of predictions was produced concerning, *e.g.* fractal decay laws and unconventional dynamical scaling. The crucial point was the suggestion that the evolution of glassy dynamics manifests itself in a dynamical window of several-orders-of-magnitude variations of time t or frequency ω adjacent to the short-time or high-frequency regime, respectively, where conventional condensed-matter dynamics is observed. Thus the mode-coupling theory (MCT) for the evolution of glassy dynamics provided motivation for studies of the dynamical regime indicated.

According to Götze[213] the recent tests of the mode-coupling theory have shown that the universal leading-order asymptotic results of the mode-coupling theory provide a complete semi-quantitative description of the evolution of structural relaxation within the GHz band for some extensively studied typical glass-forming systems. Also according to Cummings[218] a growing body of experimental data and computer simulation results indicates that the essential features of the dynamics of liquids approaching the liquid–glass transition are correctly contained in the mode-coupling theory, at least for temperatures above T_c. Elaboration of the theory for $T < T_c$ remains to be pursued in the future. See also Baschnagel,[219] Fuchs and Voigtmann,[220] Kawasaki,[221–224] Sellitto[225] and Wiedersich *et al.*[226]

Interpretation of glass transition phenomena in the light of the strength–fragility concept was recently discussed by Hutchinson.[227] As it was shown above, near the glass transition temperature the viscosity increases continuously but rapidly with cooling. As the glass forms, the molecular relaxation time increases with an Arrhenius-like (simple activated) form in some liquids, but shows highly non-Arrhenius behavior in others. The former were said to be 'strong' liquids and the latter 'fragile', *cf.* Angell *et al.*[228] and Ito *et al.*[229]

According to Hutchinson[227] an important aspect of the representation of the behavior of glass-forming liquids is that fragile liquids, as a consequence of their non-Arrhenius temperature dependence, can display very high apparent activation energies at T_g. An extensive compilation of fragilities for many glass-forming systems, evaluated by a wide variety of techniques, is given by Bohmer *et al.*[230]

This strength–fragility concept has captured the imagination of many workers in the field of relaxation kinetics. It is stressed,[227] however, that the concept relates to the temperature dependence of the viscosity or average relaxation time in the *equilibrium liquid.* The interpretation of glass-transition phenomena and of glassy-state relaxation behavior within this framework requires, therefore, some extension of these ideas into the *non-equilibrium glassy state, cf.* Hutchinson.[227]

The phenomenological model discussed by Hutchinson[227] is the one[2] that has been widely used over many years to characterize relaxation in amorphous materials. The most important aspect of this model is that it includes the two essential features of glassy relaxation behavior: *non-linearity* and *non-exponentiality*. The term 'non-linearity' refers to the dependence of the relaxation time(s) on both temperature T and the structure of glass. It is recalled that Tool[231,232] defined the structure of a glass by means of the fictive temperature T_f at which it would appear to be in equilibrium if instantaneously placed there. Using this definition of the structure, a common expression to describe the temperature and structure dependence of the relaxation time(s) is:

$$\tau = \tau_0 \exp\left[\frac{x\Delta h^*}{RT} + \frac{(1-x)\Delta h^*}{RT_f}\right] \tag{133}$$

which is often referred to as the Tool–Narayanaswamy–Moynihan[231-235] equation. In this expression, τ_0 is the relaxation time at infinite temperature, Δh^* is the apparent activation energy, and x is the nonlinearity parameter ($0 \leq x \leq 1$), which determines the relative contributions of temperature and structure to the relaxation time(s). For the use of the model, see *e.g.* Sartor and Johari[236] and Simon and McKenna.[237] For calculation of Adam–Gibbs 'primary' activation energies from published x and Δh^* parameters see Hodge and O'Reilly.[238]

It is also well known, particularly since the classic dilatometric work of Kovacs,[239] that a single relaxation time is unrealistic; glassy relaxation behavior in practice depends on a distribution of relaxation times. This may be described either, as in the model of Kovacs *et al.*,[240] as a discrete distribution or more commonly, because of its greater mathematical simplicity, by means of the stretched-exponential function (21).

Examination of the results collected by Hutchinson[227] shows some clear correlations. In particular, decreasing x is correlated with decreasing β and with increasing Δh^*. Because large values of apparent activation energy Δh^* are associated with fragile behavior, one may deduce from these correlations that small x and small β are likewise associated with fragile behavior. In other words, fragile liquids form glasses for which the relaxation is highly nonlinear (small x) and fragile liquids have a wide distribution of relaxation times (small β). Hutchinson[227] concludes that the phenomenological model for the kinetics of glassy-state relaxation, based upon eqn. (133) and a distribution of relaxation times, provides a good description of the common phenomena associated with the glass transition. See also Hutchinson *et al.*[44]

Characteristic temperatures of liquid–glass transition were discussed by Kokshenev.[241] He treats the liquid-to-glass transition as a sequence of self-similar 'smeared' ideal transitions emerging at characteristic temperatures T_0, T_g and T_c. The characteristic temperatures (Vogel–Fulcher T_0, calorimetric T_g and cross-over T_c temperatures) are discussed through the Vogel–Fulcher–Tammann equation. It is shown that their ratio is a measure of the degree of fragility m_g observed near T_g. Besides the known equation

$$T_g / T_0 = (1 - m_1 / m_g)^{-1}$$

with adjustable parameter $m = 16 \pm 2$, the equation

$$T_c T_g = (1 + m_2 m_g)/(1 - m_2 / m_g)$$

with $m_2 = 7 \pm 1$, is shown to be in accord with experiment. Based on the continuous curvature of the primary relaxation time-scale, related to m_g, the equation involving all the characteristic temperatures is introduced and the upper ($\sqrt{T_0 T_c}$) and the lower ($\sqrt[3]{T_0 T_c^2}$) estimates for the calorimetrically established characteristic temperature T_g are found. Predictions are given for characteristic temperatures T_c and fragilities m_c for a number of glass-forming liquids.

Sastry *et al.*[242] report on potential energy landscape signatures of slow dynamics in glass-forming liquids. They have studied the properties of local potential energy minima ('inherent structures') sampled by liquids at low temperatures as an approach to elucidating the mechanisms of the observed dynamical slowing down observed as the glass transition temperature is approached. This onset of slow dynamics is accompanied by the sampling of progressively deeper potential energy minima. Further, evidence is found in support of a qualitative change in the inherent structures sampled in a temperature range that includes the mode-coupling critical temperature T_c, such that a separation of vibrational relaxation within inherent structure basins from that due to inter-basin transitions becomes valid at temperatures $T < T_c$. Average inherent structure energies do not show any qualitatively significant system size dependence. See also Angell *et al.*[243] Sellitto[244] reports that kinetic lattice-gas models display fragile-glass behavior in spite of their trivial Gibbs–Boltzmann measure. This suggests that the nature of the glass transition might be, at least in some cases, understood in purely kinetic or dynamical terms. For a discussion of the glass transition within the framework of the thermodynamics of irreversible processes see Baur[245,246] and Gutzow *et al.*[247]

For thermal expansivity studies near the glass transition temperature see Bauer *et al.*,[248,249] and for time-dependent volume and enthalpy responses see Johari and Shim[250] and also McKenna and Simon.[251]

The most common situation in which physical aging is observed is when an amorphous polymer is cooled from above to below its glass transition temperature, *cf.* the previous review.[7] A constitutive model for physical aging in amorphous glassy polymers was presented by Drozdov.[252,253] See also Araki *et al.*,[254] Cerrada and McKenna,[255] and Sasaki and Nemoto.[256–258]

Reaction course in solids

Denoting by F the extent of conversion (crystallization) and using the above-mentioned formal relation $k(T) = k^{1/n}$ one can rewrite eqn. (126) as

$$g(F) = k(T)t \tag{134}$$

with

$$g(F) = [-\ln(1 - F)]^{1/n} \tag{135}$$

Furthermore, for

$$f(F) = 1/[\mathrm{d}g(F)/\mathrm{d}F] \tag{136}$$

one has

$$dF/dt = k(T)f(F) \tag{137}$$

the single-step kinetic equation used in kinetic analysis of solid-state decomposition, *cf.* Vyazovkin and Wight,[259] with $f(F)$ termed 'the reaction model'.

Several examples of reaction models, discussed by Vyazovkin and Wight[260,261] and Vyazovkin,[262] are given in Table 1. For more examples of reaction models see Dickinson and Heal[263] and Burnham.[264]

In eqn. (137) the extent of conversion, $0 \leq F \leq 1$, is a global parameter typically evaluated from mass loss or reaction heat. Using the Arrhenius equation one gets from eqn. (137)

$$dF/dt = A\exp(-E/RT)f(F) \tag{138}$$

For experiments in which samples are heated at constant rate, q, the explicit time dependence of eqn. (138) can be eliminated through the transformation

$$dF/dT = (A/q)\exp(-E/RT)f(F) \tag{139}$$

where $q = dT/dt$ is the heating rate.

For non-isothermal conditions there are several relationships used to complete the Arrhenius equation, each of which is based on an approximate form of the temperature integral that results from rearrangement and integration of eqn. (137), *i.e.*

$$\begin{aligned} g(F) &= (A/q)\int_0^{T_F} \exp(-E/RT)\,dT \\ &= I(E,T_F)/q \end{aligned} \tag{140}$$

According to Flynn[265] this temperature integral $I(E,T_F)$ has played a somewhat enigmatic role in the development of thermal analysis for reaction kinetics. It has appeared to be a necessary evil to be dealt with whenever the Arrhenius equation was integrated over time as a function of temperature. Many of the problems connected with its application have resulted from the inability to approximate the temperature

Table 1 Reaction models applied to describe thermal transformation in solids[a]

	Reaction model	$f(F)$	$g(F)$
1.	Power law	$4F^{3/4}$	$F^{1/4}$
2.	Power law	$3F^{2/3}$	$F^{1/3}$
3.	Power law	$2F^{1/2}$	$F^{1/2}$
4.	Power law	$\frac{2}{3}F^{-1/2}$	$F^{3/2}$
5.	One−dimensional diffusion	$\frac{1}{2}F^{-1}$	F^2
6.	First order	$1-F$	$-\ln(1-F)$
7.	KJMA, $n = 2$	$2(1-F)[-\ln(1-F)]^{1/2}$	$[-\ln(1-F)]^{1/2}$
8.	KJMA, $n = 3$	$3(1-F)[-\ln(1-F)]^{2/3}$	$[-\ln(1-F)]^{1/3}$
9.	KJMA, $n = 4$	$4(1-F)[-\ln(1-F)]^{3/4}$	$[-\ln(1-F)]^{1/4}$
10.	Three−dimensional diffusion	$2(1-F)^{2/3}[1-(1-F)^{1/3}]^{-1}$	$[1-(1-F)^{1/3}]^2$
11.	Contracting sphere	$3(1-F)^{2/3}$	$1-(1-F)^{1/3}$
12.	Contracting cylinder	$2(1-F)^{1/2}$	$1-(1-F)^{1/2}$

[a] Adapted from Vyazovkin and Wight[260,261] and Vyazovkin.[262]

integral accurately by a simple closed-form expression that is suitable for use in graphical form to determine the Arrhenius parameters. However, Flynn concludes that now is an opportune time to reappraise the accuracy and utility of the equations used to evaluate the temperature integral in thermal analysis kinetics. The sophistication of thermal analysis kinetics methods has advanced considerably in the past few decades and the use of computers has permitted the developments of methods for the rapid testing of the fit of experimental data to wide selections of complex kinetic models. See also Heal[266] for the evaluation of the integral of the Arrhenius function by a series of Chebyshev polynominals, and Amasaki *et al.*[267] for a simple fitting method in which, for a temperature-programmed process, instead of the equation

$$T = T_0 + qt \tag{141}$$

one uses the relation

$$1/T = 1/T_0 - \eta \ln(1+\zeta t) \tag{142}$$

where η and ζ are constants.

According to Vyazovkin and Wight[260,261] comparison of model fitting results from isothermal and non-isothermal experiments is practically meaningless. The use of model-free isoconversional methods of kinetic analysis is strongly recommended by Vyazovkin and Wight.[268] See also Sbirrazzuoli *et al.*[269]

The basic assumption of the isoconversional method is that the reaction model, as defined in eqn. (137), is not dependent on temperature or heating rate. Under isothermal conditions, we may combine eqn. (134) and the Arrhenius equation to obtain

$$-\ln t_{F,i} = \ln[A/g(F)] - E_F/RT_i \tag{143}$$

where E_F is evaluated from the slope of the plot of $-\ln t_{F,i}$ against T_i^{-1}.

For non-isothermal experiments, a nonlinear isoconversional method has been developed which avoids inaccuracies associated with analytical approximations of the temperature integral. Because $g(F)$ is independent of the heating rate, for any two experiments conducted at different heating rates, the ratio of the temperature integral $I(E,T_F)$ to the heating rate β is a constant, as shown by eqn. (140). For a set of n experiments carried out at different heating rates, the activation energy can be determined at any particular value of F by finding the value of E_F for which the function

$$\sum_{i=1}^{n}\sum_{j\neq 1}^{n}\frac{I(E_F,T_{F,i})\beta_j}{I(E_F,T_{F,i})\beta_i}$$

is a minimum. The minimization procedure is repeated for each value of F to find the dependence of activation energy on conversion. See also Baitalow *et al.*[270] for the joint use of the isoconversional method and nonlinear regression analysis, and Sempere *et al.*[271] for the progress in non-parametric kinetics. Popescu *et al.*[272] have discussed the validity of the steady-state approximation in non-isothermal kinetics, and Flammersheim and Opfermann[273] have presented the formal kinetic evolution of reactions with partial diffusion control.

A detailed analysis of the applicability of several dependences commonly used for the determination of activation energies from non-isothermal measurements was

presented by Malecki *et al.*[274] The general conclusion is that none of the examined dependences should be used to determine the activation energy. However, for a rough estimation of activation energy from differential thermal analysis (DTA) experiments, the Kissinger equation can be applied according to Occam's razor. This equation, in the present notation and with T_m denoting the DTA peak, reads

$$\ln(q / T_m^2) = \text{const} - E / RT_m \quad (144)$$

For analysis of thermoluminescence glow curves see *e.g.* Kitis *et al.*[275] or Sunta *et al.*[276,277]

Kinetic descriptions of the simple bimolecular reactions in organic solids were recently reviewed by Tolkatchev.[278] According to Galwey and Brown[279] formulating chemical mechanisms for reactions of solids has turned out to be far more difficult than was foreseen in early work. The information available *e.g.* about crystolysis reactions seems to form no coherent pattern and there are no criteria for the classification of reactivities of solid reactants. There is also no accepted basis for predicting the thermal behavior of a hitherto untested solid reactant. Without some sort of theoretical framework, the value of data already collected is difficult to assess and comparisons with other branches of chemistry are difficult to make. For computational aspects of kinetic analysis see *e.g.* Burnham,[280] Roduit[281] and Vyazovkin.[282] Turukhin and Gorokhovsky[283] have suggested a practical approach for determination of the quantum efficiency of persistent hole burning using dispersive kinetics. Long-time-scale spectral diffusion in a polymer glass was discussed by Müller *et al.*[284] Postnikov and Vinogradov[285] report on the dispersive kinetics of chemiluminescence decay in the post-photooxidation of a polyamide.

The bimolecular kinetics of the addition of pyridine, benzofulvenone and dibenzofulvenone in pyridine matrices at 15 to 70 K have been investigated by Andraos[286] by FTIR matrix isolation spectroscopy. A detailed kinetic analysis revealed a one-to-one correspondence between the disappearance of ketenes and the appearance of the corresponding ketene-pyridine zwitterions ('ketene ylides') formed upon nucleophilic addition. Dispersive second-order kinetics were found to describe the data adequately, whereas pseudo-first-order and strict second-order kinetics did not. These results are thought to indicate that the bimolecular reaction examined takes place in a heterogeneous medium with distributions of second-order rate constants. The dispersion parameter varies from 0.35 to 0.56. These findings are thought to be consistent with the matrix model proposed by Spath and Raff[287] in which the structure of the pyridine matrix is composed of inhomogeneous fast sites where the magnitude of the true reaction rate for chemical reaction exceeds the diffusion rates of both ketene and pyridine molecules. Arrhenius and Eyring thermokinetic parameters estimated from these data reveal that the barrier for reaction under these conditions is very small (less than 1 kcal mol^{-1}) with a very large negative entropy of activation (*ca.* −80 cal K^{-1} mol^{-1}). When compared with analogous solution-phase kinetic results from laser flash photolysis experiments, it was concluded that the kinetics observed at these low-temperature conditions is largely that of matrix reorganization. This sets a lower limit for the rates and an upper limit for the activation parameters of the actual chemical reactions. Furthermore, identical magnitudes for E_A, $\Delta H^{\ddagger}$ and $\Delta S^{\ddagger}$ were found even when they are calculated from second-order rate constants based on the incorrect bimolecular model applicable to homogeneous media. It was suggested that the

technique of dynamic matrix isolation spectroscopy is not adequate to obtain chemically meaningful activation parameters in bimolecular reactions. Caveats are also pointed out concerning the experimental interpretations of nonlinear Arrhenius plots obtained in cryogenic matrices, implicit assumptions about the constancy of medium properties in the construction of Arrhenius and Eyring plots, and the calculation of thermokinetic parameters from data fits to linear forms of the Arrhenius and Eyring equations.

Privalko *et al.*[288] have studied the α relaxation of a series of ether-ketone model compounds to quantity the effect of molecular stiffness on the dispersion parameter. The obtained values decrease with increasing stiffness and are within the theoretical bounds predicted for systems with spatial dimensionality varying from 2 to 1.

Some heterogeneous systems

Chemical reactions were traditionally treated in terms of three major parameters: the nature of the chemical bond formed between the reacting molecules; the stereochemical requirements or restrictions governing this molecular association; and the energetic profile of the reaction, *cf.* Avnir *et al.*[289] and the previous report.[2] *Heterogeneous* chemistry introduced a fourth parameter: the structure and geometry of the environment in which the reaction takes place. The geometry parameter is as important as the other three parameters, to the extent that it alone can dictate whether a reaction will take place at all. The geometry problem in chemistry had been unapproachable in the past. This has been changed for good. Fractal geometry has provided the proper language and the necessary vocabulary to reformulate some classical problems in heterogeneous chemistry, and the crucial importance of being able to do so for scientific progress cannot be underestimated. The origin of fractals is a dynamical, not a geometrical, problem, see Bak and Creutz.[290] The examples collected by Avnir *et al.*[289] seem to indicate that the promises of fractal geometry have, at least in part, been fulfilled. See also Erdem-Senatalar and Tatlier.[291]

Agglomerations of matter which fall into the size range of clusters and ultrafine particles play a prominent role in nature and technology. Chaiken and Goodisman[292] have described a rigorous connection between a coalescence growth model employing the Smoluchowski equation and the log-normal distribution which has been used for decades to classify empirically small particle distributions. The model assumes that only binary collisional events occur, there is conservation of monomers over the lifetime of the process, the clusters can be represented using a mass fractal approach, and there are no 'magic numbers'. Numerically, it is easy to account for the effects of evaporation, magic numbers, other inhomogeneities and possibly a non-conservative process. The model correctly incorporates the existence of multiple kinetic pathways for producing almost all cluster sizes. The properties of elemental cluster size distributions can apparently be related to the nature of the monomers as represented by the Periodic Table. The model classified cluster size distributions on the basis of a single scaling parameter which itself is a function of the dimensionality of the space in which the coalescence process occurs, the fractal dimensionality of the clusters, the fractal dimensionality of the trajectories of the agglomerating species between collisions, and the scaling of the cluster velocities with increasing cluster size. For

stochastics of aggregation see Ben Naim and Krapivsky[293] and Krapivsky and Ben-Naim.[294]

Schaaf *et al.*[295] have given a general view of irreversible deposition processes. It is interesting to find that, for hard spheres, the random sequential adsorption kinetics near the jamming limit (asymptotic regime) follows the power law[296,297]

$$\Theta(\infty) - \Theta(t) \sim t^{-1/d} \tag{145}$$

where Θ is the surface coverage, $d = 2$ and $\Theta(\infty) \sim 0.547$, *cf.* Hinrichsen *et al.*[298] The power law is a consequence of the structure of the available surface near the jamming limit, which is composed of extremely small isolated areas (much smaller than the area covered by a particle), called targets. These targets disappear due to adsorption at a rate which is proportional to their size, the larger ones disappearing first. Thus, this power law is of purely statistical and geometric nature.

Extensive EPR studies on trapped hydrogen atoms in acidic ices upon γ-irradiation at low temperatures revealed that the reactivity of these atoms at a given temperature decreases with time and depends upon the temperature at which they were formed.[299] The following picture was considered.[2,299] Immediately after irradiation, almost all hydrogen atoms are located in shallow traps which are present in relatively large numbers. Then, the hydrogen atoms move from trap to trap through the matrix until they encounter some reactive species with which they react and disappear, or until they encounter a relatively deep trap from which they are not able to escape quickly. The problem with accepting the above picture was in the reported[299] lack of isotope effects in the decay of hydrogen and deuterium atoms in partly deuteriated acidic glasses at temperatures 63–90 K. A check of this phenomenon resulted not only in the confirmation of the lack of isotope effects around 77 K but also in the revelation of inverse isotope effects at temperatures above 100 K, which is the onset temperature for the rapid decay of hydrogen atoms trapped in acidic glasses.

The real interest in inverse isotope effects arose, however, with their disclosure in metals for surface (Wang and Gomer,[300] Lee *et al.*[301]) and bulk diffusion (Völkl and Alefeld[302]), for bulk diffusion in metal hydrides (Dhawan and Prakesh[303]) and for the dynamics of acceptor–hydrogen complexes in semiconductors (Stavola and Cheng[304]).

Diffusion of atomic hydrogen on the surface and in the bulk of metals is nowadays seen, *cf.* Miyake *et al.*,[305] not only as a stimulating problem from a practical point of view but also as a fundamental problem of quantum mechanics, since a significant quantum effect is expected for the lightest element. At high temperature, diffusion occurs classically by thermal activation following the Arrhenius equation. When the temperature decreases down to around 100 K on metal surfaces, there is observed a classical quantum cross-over into a tunneling region where the hopping rate shows less temperature dependence. The inverse isotope effect is peculiar for the following reason. When we consider the diffusion from a microscopic point of view, an elementary process is thought to be the hopping of a particle (hydrogen) from a stable site to a neighboring site. At high temperature the particle hops classically over the potential barrier. Since the potential is the same for any isotope, mass (m) dependence comes only from the attempt frequency, which leads to the hopping rate, Γ, being proportional to $m^{-1/2}$. At low temperature, where the particle tunnels quantum-mechanically, Γ is expected to increase exponentially with decreasing m; this is easily

derived from the Wentzel–Kramers–Brillouin (WKB) approximation. Naively, we expect that at around the cross-over temperature, the mass dependence of Γ will be intermediate between the high-temperature $m^{-1/2}$ dependence and the low-temperature exponential behavior. Thus, the inverse isotope effect is unlikely to exist at any temperature. This is true if one does not take into account the dynamical effects of the host matrix on the guest movements. Accounting for the dynamical effects of host matrix within the general picture of dispersion kinetics, one finds the rationalization of the inverse isotope effects, *cf.* Plonka.[306]

The experimental data of Auerbach *et al.*,[307] depicted in the inset of Fig. 6, for diffusion of hydrogen on the W(110) surface, display two features of special interest. The first one is the transition from the so-called quantum regime, at low temperatures, to the so-called classical or thermally activated regime, at high temperature, *cf.* Chen and Ying.[308] The second one is the shift of these transition regions for the isotopes. The idea is that this shift is the origin of the inverse isotope effect, and, of course, of a narrow temperature region in which experiments are not able to display any isotope effect for a given pair of isotopes. The third feature, not displayed, *i.e.* silent in most experiments of this kind, is that in the so-called quantum regime the rate coefficients for reaction, diffusion or relaxation depend on time. The proper form for the specific reaction rate, *i.e.* the rate coefficient for reactions, is given by eqn. (26). By analogy, *cf.* Kakalios *et al.*,[309] the proper form for the diffusion coefficient is

$$D = D_0 (t / \hat{\zeta}_{\hat{\zeta}})^{\hat{\alpha}-1} \tag{146}$$

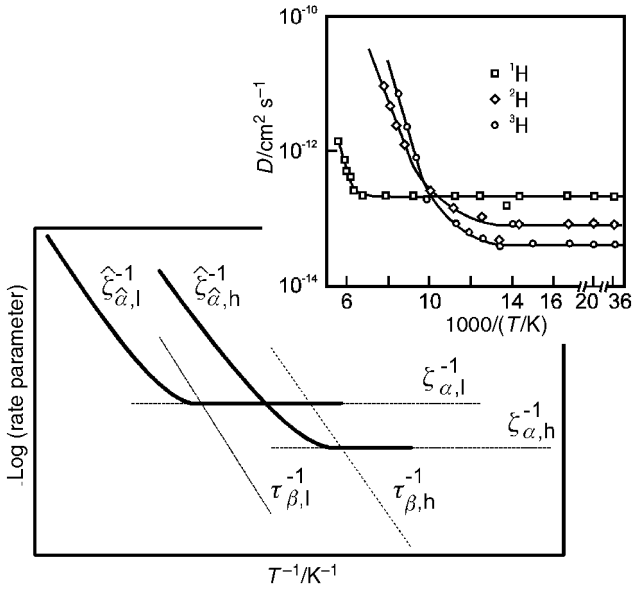

Fig. 6 Arrhenius plot of rate parameters for light, l, and heavy, h, isotopes in condensed media in the vicinity of a cooperative transition. Inset: experimental data from Auerbach *et al.*[307] Details in text.

and one has to take the data in the inset of Fig. 6 as instantaneous ones, for some value of t. They are quite adequate for illustrative purposes.

In condensed media the transitions from a low-temperature, dispersive, regime to the high-temperature one, in which classical kinetics is a valid approximation, are endemic for reactive species, *cf.* the previous review.[2] In terms of eqns. (23) and (24) these changes are rationalized by the increase of the numerical value of β from some constant value, of about 0.3 in most cases, to 1 in the transition region which is located in the vicinity of the point where ζ_α and τ_β intersect. To adapt this kinetic scheme for a rationalization of the inverse isotope effect, of the kind presented in the inset of Fig. 6, one has to take ζ_α as a temperature-independent parameter, proper for quantum-mechanical tunneling for light and heavy isotopes, $\zeta_{\alpha,\mathrm{l}}$ and $\zeta_{\alpha,\mathrm{h}}$, respectively. Here, 'proper' means hindered to some substantial degree. The reason is the self-trapping distortion, *cf.* Cheng and Stavola,[310] that localizes the trapped species at specific sites, and because the neighboring sites are inequivalent, it prevents simple tunneling. Thermal fluctuations, to be recognized as τ_0, give rise to a coincidence geometry in which tunneling from site to site can occur. These thermal fluctuations are to be different for light, $\tau_{\beta,\mathrm{l}}$, and heavy, $\tau_{\beta,\mathrm{h}}$, isotopes, *cf.* Cannelli *et al.*[311] Here, 'different' means a difference in both the pre-exponential factor and the activation energy.

The break points in the Arrhenius plot, depicted in Fig. 6, have been modeled in the following way. For each isotope, light or heavy, there is some temperature, $T_{\mathrm{c,l}}$ and $T_{\mathrm{c,h}}$, at which, in the Arrhenius plot, the τ_β^{-1} and ζ_α^{-1} lines intersect. In the temperature range 1.1–1.3, in T/T_c units, the parameter β increases linearly with temperature within the limits 0.3–1. To suppress the renewals, as rationalized above, these changes are extrapolated to $\beta = 0$. With these changes of β, the numerical values of $\hat{\alpha}$, eqn. (23), are in the range $[\alpha,1]$. Taking $\alpha = 0.3$ as a reasonable approximation for a hydrogen atom reaction or diffusion, one can calculate

$$\hat{\zeta}_{\hat{\alpha},\mathrm{l}} = \min(\hat{\zeta}_{\hat{\alpha},\mathrm{l}}, \zeta_{\alpha,\mathrm{l}}) \tag{147}$$

and

$$\hat{\zeta}_{\hat{\alpha},\mathrm{h}} = \min(\hat{\zeta}_{\hat{\alpha},\mathrm{h}}, \zeta_{\alpha,\mathrm{h}}) \tag{148}$$

which are depicted in Fig. 6 for some arbitrary sets of $\zeta_{\alpha,\mathrm{l}}$, $\tau_{\beta,\mathrm{l}}$ and $\zeta_{\alpha,\mathrm{h}}$, $\tau_{\beta,\mathrm{h}}$ values.

Thus, the break points in the Arrhenius plots do not manifest the transitions from a quantum-mechanical tunneling to a thermal overbarrier crossing but rather show the onset of host matrix dynamics that is thermally activated. Essentially, this is an onset of thermally assisted tunneling which for heavier isotopes starts at lower temperatures, *cf.* Auerbach *et al.*,[307] Cheng and Stavola.[310] See also Sun *et al.*[312] for vibrational energy relaxation rates of hydrogen isotope stretching modes.

Anomalous tracer diffusion in film-forming colloidal dispersions has been discussed by Bartsch *et al.*[313] Film-forming colloidal dispersions can be conceived as a material composed of interpenetrating hydrophobic (polymer) and hydrophilic (partially broken interfaces) phases where the transport of one phase is influenced by the geometric confinement effect imposed by the other. They have studied the transport of film-forming colloidal dispersions by introducing hydrophobic dye molecules into the colloidal particles and determining their motion with forced Rayleigh scattering as a function of length scale (grating distance Λ) and water content. At water contents between 18 and 3 wt.% they have found signatures of

anomalous tracer diffusion, namely stretched-exponential decay curves with relaxation times which deviate significantly from the q^2 dependence ($q^2 = 4\pi^2/\Lambda^2$) of Fickian diffusion. The form of the q dependence is contrary to what could be expected from a simple confinement model. Analyzing the results in terms of a length-scale-dependent effective diffusion coefficient they have found that diffusion on large length scales proceeds faster than on small length scales by nearly one order of magnitude. They have attempted to interpret their findings in a simple two-state model with enhanced diffusion on large length scales due to the existence of interconnected hydroplasticized regions.

5 Conclusions and future prospects

The research on dispersive rate processes in condensed media continues to expand in scientific scope and in its impact on scientific activity in numerous areas of studies.

The concept of renewal turned out to be a powerful way to account for matrix dynamics in reaction kinetics in condensed media. The idea to impose upon the static disorder model the additional assumption that at certain random instants reinitialization occurs, consisting in a random reassignment of the initial conditions for the reaction, results in a time-dependent specific reaction rate used in the vast areas of dispersive kinetics. Its particular form introduces the fractal time into the kinetic equation. So far, mainly stochasticity leading to fractal time equations was explored. However, the once abstract notions of fractal space and time now appear naturally in chaotic dynamic systems and there is a chance for a new insight into the dynamics of chemical systems. This new insight is needed as the concept of reaction path seems to be a somewhat artificial chemical instrument encountering troubles with formulation of the theory of thermally activated crossing of the potential energy barrier. Also, despite the great utility of the concept of renewals one may expect to have a proper dynamical model giving directly the time-scale dependence of the dispersion parameter. In such a model there might be also a place to account for the local probability of reaction, when two reactants collide, the marked decrease of which is needed to erase the effects of renewals on approaching the limit of classical kinetics. For reactive species, even when classical kinetics is valid, one sees the persistent effects of reactant reactivity restoration. These effects include viscosity dependence of the specific reaction rate, numerous forms of the compensation law and the inverse isotope effects.

Acknowledgements

I would like to thank Professor Graham Webb for his suggestion that I write this review. Special thanks go to my son, Wojciech, for his skilful computer assistance in preparation of the review, and to my wife, Ewa, for her invaluable assistance in all aspects and for the final form of the text. This work was partly supported by the Polish State Scientific Research Committee (KBN, Poland).

References

1 H. Scher, M. F. Shlesinger and J. T. Bendler, *Phys. Today*, 1991, January, 26.
2 A. Plonka, *Prog. React. Kin.*, 1991, **16**, 157.
3 A. Plonka, *Prog. React. Kin. Mech.*, 2000, **25**, 109.
4 A. Plonka, *Annu. Rep. Prog. Chem., Sect. C*, 1988, **85**, 47.
5 A. Plonka, *Annu. Rep. Prog. Chem., Sect. C*, 1992, **89**, 37.
6 A. Plonka, *Annu. Rep. Prog. Chem., Sect. C*, 1994, **91**, 107.
7 A. Plonka, *Annu. Rep. Prog. Chem., Sect. C*, 1997, **94**, 89.
8 V. I. Goldanskii, M. A. Kozhushner and L. I. Trakhtenberg, *Russ. Chem. Bull.*, 1997, **46**, 448.
9 V. I. Goldanskii, M. A. Kozhushner and L. I. Trakhtenberg, *J. Phys. Chem. B*, 1997, **101**, 10024.
10 A. Plonka and A. Paszkiewicz, *J. Chem. Phys.*, 1992, **96**, 1128.
11 I. M. Sokolov and A. Blumen, *J. Mol. Liq.*, 2000, **86**, 13 (Special Issue "Dynamical Processes in Condensed Molecular Systems", ed. A. Plonka).
12 I. Svare, S. W. Martin and F. Borsa, *Phys. Rev. B*, 2000, **61**, 228.
13 S. P. Das and S. Srivastava, *Phys. Lett. A*, 2000, **266**, 58.
14 J. Ross and M. O. Vlad, *Annu. Rev. Phys. Chem.*, 1999, **50**, 51.
15 V. Chernyak, M. Schultz and S. Mukamel, *J. Chem. Phys.*, 1999, **111**, 7416.
16 M. Kuno, D. P. Fromm, H. F. Hamann, A. Gallagher and D. J. Nesbitt, *J. Chem. Phys.*, 2000, **112**, 3117.
17 A. Okada, *J. Chem. Phys.*, 2000, **112**, 8595.
18 S. R. Logan, *J. Chem. Educ.*, 1982, **59**, 279.
19 R. M. Noyes, *Prog. React. Kin.*, 1961, **1**, 129.
20 S. Arrhenius, *Z. Phys. Chem.*, 1889, **4**, 226.
21 I. Marsi and L. Seres, *Chemometr. Intell. Lab. Syst.*, 2000, **50**, 53.
22 E. Urbanovici, C. Popescu and E. Segal, *J. Therm. Anal. Calorim.*, 2000, **60**, 581.
23 F. W. Wilburn, *Thermochim. Acta*, 2000, **354**, 99.
24 T. Ozawa, *Thermochim. Acta*, 2000, **355**, 35.
25 T. Ozawa, *J. Therm. Anal. Calorim.*, 2000, **60**, 887.
26 H. Suga, *Thermochim. Acta*, 2000, **355**, 69.
27 K. Nakamura, T. Takayanagi and S. Sato, *Chem. Phys. Lett.*, 1989, **160**, 295.
28 A. Barkatt, C. A. Angell and J. R. Miller, *J. Phys. Chem.*, 1978, **82**, 2143.
29 S. J. Rzad, P. P. Infelta, J. M. Warman and R. H. Schuler, *J. Chem. Phys.*, 1970, **52**, 3971.
30 A. Barkatt, M. Ottolenghi and J. Rabani, *J. Phys. Chem.*, 1973, **77**, 2857.
31 A. Barkatt and J. Rabani, *J. Phys. Chem.*, 1975, **79**, 2952.
32 W. H. Hamill, *Chem. Phys. Lett.*, 1981, **77**, 467.
33 A. A. Zavitsas, *J. Am. Chem. Soc.*, 1998, **120**, 6578.
34 H. A. Kramers, *Physica*, 1940, **7**, 284.
35 A. M. Berezhkovskii, D. J. Bicout and G. H. Weiss, *J. Chem. Phys.*, 1999, **111**, 11050.
36 J. R. Chaudhuri, B. Ch. Bag and D. S. Ray, *J. Chem. Phys.*, 1999, **111**, 10852.
37 S. K. Banik, J. R. Chaudhuri and D. S. Ray, *J. Chem. Phys.*, 2000, **112**, 8330.
38 M. L. Williams, R. F. Landel and J. D. Ferry, *J. Am. Chem. Soc.*, 1955, **77**, 3701.
39 C. A. Angell, *Polymer*, 1997, **38**, 6261.
40 J. Rault, *J. Non-Cryst. Solids*, 2000, **271**, 177.
41 J. T. Bendler, J. J. Fontanella and M. F. Shlesinger, personal communication.
42 G. Adam and J. H. Gibbs, *J. Chem. Phys.*, 1965, **43**, 139.
43 H. Huth, M. Beiner and E. Donth, *Phys. Rev. B*, 2000, **61**, 15092.
44 J. M. Hutchinson, S. Montserrat, Y. Calventus and P. Cortes, *Macromolecules*, 2000, **33**, 5252.
45 G. P. Johari, *J. Chem. Phys.*, 2000, **112**, 7518.
46 G. P. Johari, *J. Chem. Phys.*, 2000, **112**, 8958.
47 G. P. Johari, *J. Chem. Phys.*, 2000, **112**, 10957.
48 G. P. Johari, *J. Chem. Phys.*, 2000, **113**, 751.
49 G. P. Johari, *J. Mol. Struct.*, 2000, **520**, 249.
50 T. Kitamura, *Physica A*, 1999, **262**, 16.
51 L. M. Carvalho, P. Guegan, H. Cheradame and A. S. Gomes, *Eur. Polym. J.*, 2000, **36**, 401.
52 R. Hilfer and L. Anton, *Phys. Rev. E*, 1995, **51**, R848.
53 G. Mittag-Leffler, *Acta Math.*, 1905, **29**, 101.
54 E. Barkai, R. Metzler and J. Klafter, *Phys. Rev. E*, 2000, **61**, 132.
55 E. Barkai, V. Fleurov and J. Klafter, *Phys. Rev. E*, 2000, **61**, 1164.
56 E. Barkai and R. J. Silbey, *J. Phys. Chem. B*, 2000, **104**, 3866.
57 D. Kusnezov, A. Bulgac and G. D. Dang, *Phys. Rev. Lett.*, 1999, **82**, 1136.
58 A. Rocco and B. J. West, *Physica A*, 1999, **265**, 535.
59 H. Schiessel, Chr. Friedrich and A. Blumen, in *Applications of Fractional Calculus in Physics*, ed. R. Hilfer, World Scientific, Singapore, 2000.

60 G. M. Zaslavsky, *J. Plasma Phys.*, 1998, **59**, 671.
61 R. Metzler, E. Barkai and J. Klafter, *Europhys. Lett.*, 1999, **46**, 431.
62 R. Metzler, E. Barkai and J. Klafter, *Phys. Rev. Lett.*, 1999, **82**, 3563.
63 R. Metzler and J. Klafter, *J. Mol. Liq.*, 2000, **86**, 219 (Special Issue "Dynamical Processes in Condensed Molecular Systems", ed. A. Plonka).
64 I. M. Sokolov, *Phys. Rev. E*, 1999, **60**, 5528.
65 L. F. Richardson, *Proc. R. Soc. (London), Ser. A*, 1926, **110**, 709.
66 I. M. Sokolov, A. Blumen and J. Klafter, *Europhys. Lett.*, 1999, **47**, 152.
67 I. M. Sokolov, J. Klafter and A. Blumen, *Phys. Rev. E*, 2000, **61**, 2717.
68 T. Ishii, *Solid State Commun.*, 2000, **116**, 327.
69 C. Schulzky, C. Essex, M. Davison, A. Franz and K. H. Hoffmann, *J. Phys. A: Math. Gen.*, 2000, **33**, 5501.
70 R. V. Chamberlin, *Phase Transitions*, 1998, **65**, 169.
71 R. Bergman, *J. Appl. Phys.*, 2000, **88**, 1356.
72 G. Govindaraj and R. Murugaraj, *Mater. Sci. Eng. B*, 2000, **77**, 60.
73 J. C. Dyre and T. B. Schrøder, *Rev. Mod. Phys.*, 2000, **72**, 873.
74 D. L. Sidebottom, *Phys. Rev. B*, 2000, **61**, 14507.
75 T. Ishii and T. Abe, *J. Phys. Soc. Jpn.*, 1998, **67**, 505.
76 T. Ishii and T. Abe, *J. Phys. Soc. Jpn.*, 1999, **68**, 3127.
77 T. Ishii and T. Abe, *J. Phys. Soc. Jpn.*, 2000, **69**, 2549.
78 A. Plonka and W. Bogus, *Radiat. Phys. Chem.*, 1998, **53**, 639.
79 S. M. Jazwinski, *Mol. Microbiol.*, 1990, **4**, 337.
80 M. F. Shlesinger, G. M. Zaslavsky and J. Klafter, *Nature*, 1993, **363**, 31.
81 G. M. Zaslavsky, *Chaos*, 1995, **5**, 653.
82 G. M. Zaslavsky and M. Edelman, *Chaos*, 2000, **10**, 135.
83 A. Iomin and G. M. Zaslavsky, *Chaos*, 2000, **10**, 147.
84 V. Latora, A. Rapisarda and S. Ruffo, *Physica A*, 2000, **280**, 81.
85 C. K. Majumdar, *Solid State Commun.*, 1971, **9**, 1087.
86 U. Mohanty, *J. Chem. Phys.*, 1994, **100**, 5905.
87 Zh. Y. Shi and R. Kopelman, *J. Phys. Chem.*, 1992, **96**, 6858.
88 K. L. Ngai, *J. Phys.: Condens. Matter*, 1999, **11**, A119.
89 J. R. Macdonald, *J. Appl. Phys.*, 1998, **84**, 812.
90 K. L. Ngai, *Philos. Mag. B*, 1999, **79**, 1783.
91 K. L. Ngai, *J. Phys. Chem. B*, 1999, **103**, 10684.
92 K. L. Ngai, *J. Phys. IV (Fr.)*, 2000, **10**, 7.
93 K. L. Ngai, *J. Phys., Condens. Matter*, 2000, **12**, 6437.
94 K. L. Ngai, *J. Non-Cryst. Solids*, 2000, **275**, 7.
95 T. Asano and H. Sumi, *Chem. Phys. Lett.*, 1998, **294**, 493.
96 A. Ansari, *J. Chem. Phys.*, 1999, **110**, 1774.
97 J. G. McAnanama, D. A. Wasylyshyn and G. P. Johari, *Chem. Phys.*, 2000, **252**, 237.
98 O. Exner, *Prog. Phys. Org. Chem.*, 1973, **10**, 411.
99 S. Vyazovkin and C. A. Wight, *Annu. Rev. Phys. Chem.*, 1997, **48**, 125.
100 A. Plonka, *J. Mol. Struct.*, 1999, **479**, 177.
101 J. C. Phillips, *Rep. Prog. Phys.*, 1996, **59**, 1133.
102 P. Budrugeac and E. Segal, *J. Therm. Anal. Calorim.*, 1999, **56**, 835.
103 P. Budrugeac, *Polym. Degrad. Stab.*, 2000, **67**, 271.
104 A. K. Burnham and R. L. Braun, *Energy Fuels*, 1999, **13**, 1.
105 A. Plonka and A. Paszkiewicz, *Chem. Phys.*, 1996, **212**, 1.
106 A. Plonka, *J. Phys. Chem. B*, 2000, **104**, 3804.
107 K. Weron, *Acta Phys. Polon. A*, 1986, **70**, 529.
108 C. P. Lindsey and G. D. Patterson, *J. Chem. Phys.*, 1980, **73**, 3348.
109 O. Edholm and C. Blomberg, *Chem. Phys.*, 2000, **252**, 221.
110 R. Skulski, *Physica A*, 1999, **274**, 361.
111 R. Skulski, *Condens. Matter Phys.*, 1999, **2**, 661.
112 A. L. Edelstein and N. Agmon, *J. Phys. Chem.*, 1995, **99**, 5389.
113 H. Kim, S. Shin and K. J. Shin, *J. Chem. Phys.*, 1998, **108**, 5861.
114 H. Kim, S. Shin and K. J. Shin, *Chem. Phys. Lett.*, 1998, **291**, 341.
115 H. Kim and K. J. Shin, *Phys. Rev. Lett.*, 1999, **82**, 1578.
116 C. Nassif and P. R. Silva, *Mod. Phys. Lett. B*, 1999, **13**, 829.
117 N. Agmon and I. V. Gopich, *J. Chem. Phys.*, 2000, **112**, 2863.
118 M. Solc, *Z. Phys. Chem.*, 2000, **214**, 253.
119 A. V. Barzykin, K. Seki and M. Tachiya, *J. Phys. Chem. B*, 1999, **103**, 6881.
120 A. V. Barzykin, K. Seki and M. Tachiya, *J. Phys. Chem. B*, 1999, **103**, 9156.
121 S. K. Pal, D. Sukul, D. Mandal, S. Sen and K. Bhattacharyya, *Chem. Phys. Lett.*, 2000, **327**, 91.

122 W. Naumann, *J. Chem. Phys.*, 2000, **112**, 7152.
123 S. Redner and P. L. Krapivsky, *Am. J. Phys.*, 1999, **67**, 1277.
124 V. N. Kuzovkov, J. Mai, I. M. Sokolov and A. Blumen, *Phys. Rev. E*, 1999, **59**, 2561.
125 Y. Tabata and N. Kuroda, *Phys. Rev. B*, 2000, **61**, 3085.
126 H. Kim and K. J. Shin, *J. Chem. Phys.*, 2000, **112**, 8312.
127 A. A. Kipriyanov, O. A. Igoshin and A. B. Doktorov, *Physica A*, 1999, **268**, 567.
128 O. A. Igoshin, A. A. Kipriyanov and A. B. Doktorov, *Chem. Phys.*, 1999, **244**, 371.
129 A. A. Kipriyanov, O. A. Igoshin and A. B. Doktorov, *Physica A*, 2000, **275**, 99.
130 J. Sung and S. Lee, *J. Chem. Phys.*, 1999, **111**, 796.
131 J. Sung, J. Chi and S. Lee, *J. Chem. Phys.*, 1999, **111**, 804.
132 J. Sung and S. Lee, *J. Chem. Phys.*, 1999, **111**, 10159.
133 J. Sung and S. Lee, *J. Chem. Phys.*, 2000, **112**, 2128.
134 O. Benichou, M. Moreau and G. Oshanin, *Phys. Rev. E*, 2000, **61**, 3388.
135 T. Bandyopadhyay, K. Seki and M. Tachiya, *J. Chem. Phys.*, 2000, **112**, 2849.
136 R. Graber, *Physica A*, 1999, **271**, 223.
137 V. M. Syutkin, *Chem. Phys.*, 1999, **248**, 213.
138 A. Blumen, I. Sokolov, G. Zumofen and J. Klafter, in *Computational Physics*, ed. K. H. Hoffmann and M. Schreiber, Springer, Berlin, 1996, p. 102.
139 S. Nechaev, G. Oshanin and A. Blumen, *J. Stat. Phys.*, 2000, **98**, 281.
140 B. Ilan and R. F. Loring, *J. Chem. Phys.*, 2000, **112**, 10588.
141 H. Kim and K. J. Shin, *Phys. Rev. E*, 2000, **61**, 3426.
142 A. R. Dinner and M. Karplus, *J. Phys. Chem. B*, 1999, **103**, 7976.
143 R. Du, V. S. Pande, A. Yu. Grosberg, T. Tanaka and E. Shakhnovich, *J. Chem. Phys.*, 1999, **111**, 10375.
144 A. Fernández, A. Colubri, T. Burastero and A. Tablar, *Phys. Chem. Chem. Phys.*, 1999, **1**, 4347.
145 H. Kim, M. Yang and K. J. Shin, *J. Chem. Phys.*, 1999, **110**, 3946.
146 S. Yang, J. Kim and S. Lee, *J. Chem. Phys.*, 1999, **111**, 10119.
147 R. H. Callender, R. B. Dyer, R. Gilmanshin and W. H. Woodruff, *Annu. Rev. Phys. Chem.*, 1998, **49**, 173.
148 M. Gruebele, *Annu. Rev. Phys. Chem.*, 1999, **50**, 485.
149 J. Wang and W. Wang, *Nat. Struct. Biol.*, 1999, **6**, 1033.
150 J. Wang and W. Wang, *Phys. Rev. E*, 2000, **61**, 6981.
151 A. Fernández and S. Berry, *J. Chem. Phys.*, 2000, **112**, 5212.
152 A. Fernández, K. S. Kostov and R. S. Berry, *J. Chem. Phys.*, 2000, **112**, 5223.
153 E. Pitard and H. Orland, *Europhys. Lett.*, 2000, **49**, 169.
154 S.-R. Yeh, S. Han and D. L. Rousseau, *Acc. Chem. Res.*, 1998, **31**, 727.
155 A. Eaton, V. Munoz, P. A. Thompson, E. R. Henry and J. Hofrichter, *Acc. Chem. Res.*, 1998, **31**, 745.
156 J. Sabelko, J. Ervin and M. Gruebele, *Proc. Natl. Acad. Sci.*, 1999, **96**, 6031.
157 W. Y. Yang, R. B. Prince, J. Sabelko, J. S. Moore and M. Gruebele, *J. Am. Chem. Soc.*, 2000, **122**, 3248.
158 F. Parak and K. Achterhold, *Hyperfine Interact.*, 1999, **123**/**124**, 825.
159 V. E. Prusakov, D. C. Lamb, F. G. Parak and V. I. Goldanskii, *Chem. Phys. Rep.*, 1999, **18**, 835.
160 M. Volk, Yu. Kholodenko, H. S. M. Lu, E. A. Gooding, W. F. DeGrado and R. M. Hochstrasser, *J. Phys. Chem. B*, 1997, **101**, 8607.
161 R. Metzler, J. Klafter, J. Jortner and M. Volk, *Chem. Phys. Lett.*, 1998, **293**, 477.
162 G. R. Palmer, D. L. Stein, E. Abrahams and P. W. Anderson, *Phys. Rev. Lett.*, 1984, **53**, 958.
163 C. A. Angell, *Physica D*, 1997, **107**, 122.
164 M. Oliveberg, *Acc. Chem. Res.*, 1998, **31**, 765.
165 J. Heidel and J. Maloney, *J. Aust. Math. Soc. Ser. B*, 2000, **41**, 410.
166 P. G. Wolynes, *Nature*, 1996, **382**, 495.
167 H. Suga, *J. Therm. Anal. Calorim.*, 2000, **60**, 957.
168 R. A. Ramos, P. A. Rokvold and M. A. Novotny, *Phys. Rev. B*, 1999, **59**, 9053.
169 M. Fanfoni and M. Tomellini, *Nuovo Cimento*, 1998, **20D**, 1171.
170 A. Korobov, *J. Math. Chem.*, 1998, **24**, 261.
171 M. C. Weinberg, D. P. Birnie III and V. A. Shneidman, *J. Non-Cryst. Solids*, 1997, **219**, 89.
172 P. Supaphol and J. E. Spruiell, *J. Appl. Polym. Sci.*, 2000, **75**, 44.
173 P. Supaphol and J. E. Spruiell, *J. Macromol. Sci.–Phys.*, 2000, **B39**, 257.
174 M. C. Tobin, *J. Polym. Sci., Polym. Phys. Ed.*, 1977, **15**, 2269.
175 A. Ya. Malkin, V. P. Beghishev, I. A. Keapin and S. A. Bolgov, *Polym. Eng. Sci.*, 1984, **24**, 1396.
176 P. Supaphol, *J. Appl. Polym. Sci.*, 2000, **78**, 338.
177 J. R. Frade, *J. Am. Ceram. Soc.*, 1998, **81**, 2654.
178 M. Lambrigger, *Polym. J.*, 1998, **30**, 262.
179 M. Lambrigger, *Polym. Eng. Sci.*, 1998, **38**, 610.
180 A. L. Oliveira, J. M. Oliveira, R. N. Correia, M. H. V. Fernandes and J. R. Frade, *J. Am. Ceram. Soc.*, 1998, **81**, 3270.
181 K. Nakamura, T. Watanabe, K. Katayama and T. Amano, *J. Appl. Polym. Sci.*, 1972, **16**, 1077.

182 K. Nakamura, K. Katayama and T. Amano, *J. Appl. Polym. Sci.*, 1973, **17**, 1031.
183 K. Nakamura, T. Watanabe, T. Amano and K. Katayama, *J. Appl. Polym. Sci.*, 1974, **18**, 615.
184 K. P. Chuah, S. N. Gan and K. K. Chee, *Polymer*, 1998, **40**, 253.
185 M. G. Lu, M. J. Shim and S. W. Kim, *J. Therm. Anal. Calorim.*, 1999, **58**, 701.
186 O. Grong and O. R. Myhr, *Acta Mater.*, 2000, **48**, 445.
187 J. Málek, A. Watanabe and T. Mitsuhashi, *J. Therm. Anal. Calorim.*, 2000, **60**, 699.
188 J. A. Martins and J. J. C. Cruz-Pinto, *Polymer*, 2000, **41**, 6875.
189 J. Vázquez, P. L. Lopez-Alemany, P. Villares and R. Jimenez-Garay, *J. Phys. Chem. Solids*, 2000, **61**, 493.
190 G. Carter, *Philos. Mag. A*, 1999, **79**, 2773.
191 J. Málek, *J. Therm. Anal. Calorim.*, 1999, **56**, 763.
192 J. Málek, *Thermochim. Acta*, 2000, **355**, 239.
193 M. Avrami, *J. Chem. Phys.*, 1939, **7**, 1103.
194 M. Avrami, *J. Chem. Phys.*, 1940, **8**, 212.
195 M. Avrami, *J. Chem. Phys.*, 1941, **9**, 177.
196 M. Fanfoni, R. Polini, V. Sessa, M. Tomellini and M. Volpe, *Appl. Surf. Sci.*, 1999, **152**, 126.
197 M. Tomellini and M. Fanfoni, *Surf. Sci.*, 2000, **450**, L267.
198 M. Tomellini and M. Fanfoni, *Surf. Sci.*, 1996, **349**, L191.
199 E. Pineda and D. Crespo, *Phys. Rev. B*, 1999, **60**, 3104.
200 M. Volpe, M. Tomellini and M. Fanfoni, *Surf. Sci.*, 1999, **423**, L258.
201 C. A. Angell, *Curr. Opin. Solid State Mater. Sci.*, 1996, **1**, 578.
202 P. Lunkenheimer, U. Schneider, R. Brand and A. Loidl, *Contemp. Phys.*, 2000, **41**, 15.
203 C. A. Angell, *J. Phys.: Condens Matter*, 2000, **12**, 6463.
204 C. A. Angell, K. L. Ngai, G. B. McKenna, P. F. McMillan and S. W. Martin, *J. Appl. Phys.*, 2000, **88**, 3113.
205 M. D. Ediger, *Annu. Rev. Phys. Chem.*, 2000, **51**, 99.
206 E. Hempel, G. Hempel, A. Hensel, C. Schick and E. Donth, *J. Phys. Chem. B*, 2000, **104**, 2460.
207 E. Donth, E. Hempel and S. Schick, *J. Phys.: Condens. Matter*, 2000, **12**, L281.
208 C.-Y. Wang and M. D. Ediger, *J. Phys. Chem. B*, 2000, **104**, 1724.
209 M. Russina, F. Mezei, R. Lechner, S. Longeville and B. Urban, *Phys. Rev. Lett.*, 2000, **84**, 3630.
210 C.-Y. Wang and M. D. Ediger, *J. Chem. Phys.*, 2000, **112**, 6933.
211 B. Schiener, R. Böhmer, A. Loidl and R. V. Chamberlin, *Science*, 1996, **274**, 752.
212 H. Sillescu, *J. Phys.: Condens. Matter*, 1999, **11**, A271.
213 W. Götze, *J. Phys.: Condens. Matter*, 1999, **11**, A1.
214 A. Huwe, F. Kremer, P. Behrens and W. Schwieger, *Phys. Rev. Lett.*, 1999, **82**, 2338.
215 F. Kremer, A. Huwe, M. Arndt, P. Behrens and W. Schwieger, *J. Phys.: Condens. Matter*, 1999, **11**, A175.
216 K. L. Ngai, *J. Therm. Anal. Calorim.*, 1999, **57**, 745.
217 M.-C. Bellissent-Funel, *J. Mol. Liq.*, 2000, **84**, 39.
218 H. Z. Cummings, *J. Phys.: Condens. Matter*, 1999, **11**, A95.
219 J. Baschnagel, in *Structure and Properties of Glassy Polymers, Proc. ACS Symp. Ser. 710*, ed. M. R. Tant and A. J. Hill, Americal Chemical Society, Washington, DC, 1998, p. 53.
220 M. Fuchs and Th. Voigtmann, *Philos. Mag. B*, 1999, **79**, 1799.
221 K. Kawasaki, *Nuovo Cimento*, 1998, **20D**, 2325.
222 K. Kawasaki, *Jpn. J. Appl. Phys.*, 1998, **37**, 36.
223 K. Kawasaki, *J. Phys.: Condens. Matter*, 2000, **12**, 6343.
224 K. Kawasaki, *Physica A*, 2000, **281**, 348.
225 M. Sellitto, *Eur. Phys. J. B*, 1998, **4**, 135.
226 J. Wiedersich, N. V. Surovtsev and E. Rössler, *J. Chem. Phys.*, 2000, **113**, 1143.
227 J. M. Hutchinson, *Polym. Int.*, 1998, **47**, 56.
228 C. A. Angell, B. E. Richards and V. Velikov, *J. Phys.: Condens. Matter*, 1999, **11**, A75.
229 K. Ito, C. T. Moynihan and A. Angell, *Nature*, 1999, **398**, 492.
230 R. Bohmer, K. L. Ngai, C. A. Angell and D. J. Plazek, *J. Chem. Phys.*, 1993, **99**, 4201.
231 A. Q. Tool and C. G. Eichlin, *J. Am. Ceram. Soc.*, 1931, **14**, 276.
232 A. Q. Tool, *J. Am. Ceram. Soc.*, 1948, **31**, 177.
233 A. Q. Tool, *J. Am. Ceram. Soc.*, 1946, **29**, 240.
234 O. S. Narayanaswamy, *J. Am. Ceram. Soc.*, 1971, **54**, 491.
235 C. T. Moynihan, A. J. Eastel, M. A. DeBolt and J. Trucker, *J. Am. Ceram. Soc.*, 1976, **59**, 12.
236 G. Sartor and G. P. Johari, *J. Phys. Chem. B*, 1999, **103**, 11 036.
237 S. L. Simon and G. B. McKenna, *Thermochim. Acta*, 2000, **348**, 77.
238 I. M. Hodge and J. M. O'Reilly, *J. Phys. Chem. B*, 1999, **103**, 4171.
239 A. J. Kovacs, *Fortschr. Hochpolym. Forsch.*, 1964, **3**, 394.
240 A. J. Kovacs, J. J. Aklonis, J. M. Hutchinson and A. R. Ramos, *J. Polym. Sci., Polym. Phys. Ed.*, 1979, **17**, 1097.
241 V. B. Kokshenev, *Physica A*, 1999, **262**, 88.

242 S. Sastry, P. G. Debenedetti, F. H. Stillinger, T. B. Schröder, J. C. Dyre and S. C. Glotzer, *Physica A*, 1999, **270**, 301.
243 C. A. Angell, J. L. Green, K. Ito, P. Lucas and B. E. Richards, *J. Therm. Anal. Calorim.*, 1999, **57**, 717.
244 M. Sellitto, *J. Phys.: Condens. Matter*, 2000, **12**, 6477.
245 H. Baur, *Z. Naturforsch.*, 1998, **53A**, 157.
246 H. Baur, *Z. Naturforsch.*, 2000, **55A**, 641.
247 I. Gutzow, D. Ilieva, F. Babalievski and V. Yamakov, *J. Chem. Phys.*, 2000, **112**, 10941.
248 C. Bauer, R. Richert, R. Böhmer and T. Christensen, *J. Non-Cryst. Solids*, 2000, **262**, 276.
249 C. Bauer, R. Böhmer, S. Moreno-Flores, R. Richert and H. Sillescu, *Phys. Rev. E*, 2000, **61**, 1755.
250 G. P. Johari and J. G. Shim, *J. Non-Cryst. Solids*, 2000, **261**, 52.
251 G. B. McKenna and S. L. Simon, in *Time Dependent and Nonlinear Effects in Polymers and Composites*, ASTM STP 1357, ed. R. A. Schapery and C. T. Sun, American Society for Testing and Materials, West Conshohocken, PA, 2000, p. 18.
252 A. D. Drozdov, *Model. Simul. Mater. Sci. Eng.*, 1999, **7**, 1045.
253 A. D. Drozdov, *Comput. Mater. Sci.*, 2000, **18**, 48.
254 O. Araki, T. Yoshizawa, T. Takigawa and T. Masuda, *Polym. J.*, 2000, **32**, 97.
255 M. L. Cerrada and G. B. McKenna, in *Time Dependent and Nonlinear Effects in Polymers and Composites*, ASTM STP 1357, ed. R. A. Schapery and C. T. Sun, American Society for Testing and Materials, West Conshohocken, PA, 2000, p. 47.
256 M. Sasaki and K. Nemoto, *J. Phys. Soc. Jpn.*, 2000, **69**, 2283.
257 M. Sasaki and K. Nemoto, *J. Phys. Soc. Jpn.*, 2000, **69**, 2642.
258 M. Sasaki and K. Nemoto, *J. Phys. Soc. Jpn.*, 2000, **69**, 3045.
259 S. Vyazovkin and C. A. Wight, *Thermochim. Acta*, 1999, **340–341**, 53.
260 S. Vyazovkin and C. A. Wight, *J. Phys. Chem. A*, 1997, **101**, 8279.
261 S. Vyazovkin and C. A. Wight, *Int. Rev. Phys. Chem.*, 1998, **17**, 407.
262 S. Vyazovkin, *Int. Rev. Phys. Chem.*, 2000, **19**, 45.
263 C. F. Dickinson and G. R. Heal, *Thermochim. Acta*, 1999, **340–341**, 89.
264 A. K. Burnham, *J. Therm. Anal. Calorim.*, 2000, **60**, 895.
265 J. H. Flynn, *Thermochim. Acta*, 1997, **300**, 83.
266 G. R. Heal, *Thermochim. Acta*, 1999, **340–341**, 69.
267 I. Amasaki, Z. Gao and M. Nakada, *Chem. Lett.*, 2000, 520.
268 S. Vyazovkin and C. A. Wight, *Anal. Chem.*, 2000, **72**, 3171.
269 N. Sbirrazzuoli, L. Vincent, J. Bouillard and L. Elegant, *J. Therm. Anal. Calorim.*, 1999, **56**, 783.
270 F. Baitalow, H.-G. Schmidt and G. Wolf, *Thermochim. Acta*, 1999, **337**, 111.
271 J. Sempere, R. Nomen and R. Serra, *J. Therm. Anal. Calorim.*, 1999, **56**, 843.
272 C. Popescu, E. Urbanovici and E. Segal, *J. Therm. Anal. Calorim.*, 1999, **58**, 677.
273 H. J. Flammersheim and J. Opfermann, *Thermochim. Acta*, 1999, **337**, 141.
274 A. Malecki, B. Prochowska-Klisch and K. T. Wojciechowski, *J. Therm. Anal.*, 1998, **54**, 399.
275 G. Kitis, J. M. Gomez-Ros and J. W. N. Tuyn, *J. Phys. D: Appl. Phys.*, 1998, **31**, 2636.
276 C. M. Sunta, R. N. Kulkarni, T. M. Piters, W. E. F. Ayta and S. Watanabe, *J. Phys. D: Appl. Phys.*, 1998, **31**, 2074.
277 C. M. Sunta, W. E. F. Ayta, T. M. Piters, R. N. Kulkarni and S. Watanabe, *J. Phys. D: Appl. Phys.*, 1999, **32**, 1271.
278 V. A. Tolkatchev, in *Reactivity of Molecular Solids*, ed. E. Boldyreva and V. Boldyrev, John Wiley & Sons, Chichester, 1999, p. 175.
279 A. K. Galwey and M. E. Brown, *J. Therm. Anal. Calorim.*, 2000, **60**, 863.
280 A. K. Burnham, *Thermochim. Acta*, 2000, **355**, 165.
281 B. Roduit, *Thermochim. Acta*, 2000, **355**, 171.
282 S. Vyazovkin, *Thermochim. Acta*, 2000, **355**, 155.
283 A. V. Turukhin and A. A. Gorokhovsky, *Chem. Phys. Lett.*, 2000, **317**, 109.
284 J. Müller, H. Maier, G. Hannig, O. V. Khodykin, D. Haarer and B. M. Kharlamov, *J. Chem. Phys.*, 2000, **113**, 876.
285 L. M. Postnikov and A. V. Vinogradov, *Polym. Sci., Ser. A*, 2000, **42**, 493.
286 J. Andraos, *J. Phys. Chem. A*, 2000, **104**, 1532.
287 B. W. Spath and L. M. Raff, *J. Phys. Chem.*, 1992, **96**, 2179.
288 V. P. Privalko, T. A. Ezquerra, M. Zolotukhin, F. J. Balta-Calleja, G. Nequlqueo, C. Garcia, J. G. de la Campa and J. de Abajo, *J. Chem. Phys.*, 2000, **112**, 5254.
289 D. Avnir, R. Gutfraind and D. Farin, in *Fractals in Science*, ed. A. Bunde and S. Havlin, Springer-Verlag, Berlin, 1994, p. 229.
290 P. Bak and M. Creutz, in *Fractals in Science*, ed. A. Bunde and S. Havlin, Springer-Verlag, Berlin, 1994, p. 26.
291 A. Erdem-Senatalar and M. Tatlier, *Chaos, Solitons Fractals*, 2000, **11**, 953.
292 J. Chaiken and J. Goodisman, *J. Photochem. Photobiol. A: Chem.*, 1994, **80**, 53.

293 E. Ben-Naim and P. L. Krapivsky, *J. Phys. A: Math. Gen.*, 2000, **33**, 5477.
294 P. L. Krapivsky and E. Ben-Naim, *J. Phys. A: Math. Gen.*, 2000, **33**, 5465.
295 P. Schaaf, J.-C. Voegel and B. Senger, *J. Phys. Chem. B*, 2000, **104**, 2204.
296 Y. J. Pomeau, *J. Phys. A*, 1980, **13**, L193.
297 R. H. Swendsen, *Phys. Rev. A*, 1981, **24**, 504.
298 E. L. Hinrichsen, J. Feder and T. Jøssang, *J. Stat. Phys.*, 1986, **44**, 793.
299 J. Kroh and A. Plonka, *J. Phys. Chem.*, 1975, **79**, 2600.
300 S. C. Wang and R. Gomer, *J. Chem. Phys.*, 1985, **83**, 4193.
301 A. Lee, X. D. Zhu, L. Deng and U. Linke, *Phys. Rev. B: Condens. Matter*, 1992, **46**, 15 472.
302 J. Völkl and G. Alefeld, *Top. Appl. Phys., Hydrogen Met.*, 1978, **1**, 321.
303 L. L. Dhawan and S. Prakesh, *Phys. Rev. B*, 1984, **29**, 3661.
304 M. Stavola and Y. M. Cheng, *Solid State Commun.*, 1995, **93**, 431.
305 T. Miyake, K. Kusakabe and S. Tsuneyuki, *Surf. Sci.*, 1996, **363**, 403.
306 A. Plonka, *Nukleonika*, 1998, **43**, 415.
307 A. Auerbach, K. F. Freed and R. Gomer, *J. Chem. Phys.*, 1987, **86**, 2356.
308 L. Y. Chen and S. C. Ying, *Phys. Rev. Lett.*, 1994, **73**, 700.
309 J. Kakalios, R. A. Street and W. B. Jackson, *Phys. Rev. Lett.*, 1987, **59**, 1037.
310 Y. M. Cheng and M. Stavola, *Phys. Rev. Lett.*, 1994, **73**, 3419.
311 G. Cannelli, R. Cantelli, F. Cordero and F. Trequattrini, *J. Phys. IV (Fr.)*, 1996, **6**, C813.
312 Y.-C. Sun, H.-F. Lu and M.-S. Ho, *Chem. Phys. Lett.*, 2000, **318**, 7.
313 E. Bartsch, T. Jahr, A. Veniaminov and H. Sillescu, *J. Phys. IV (Fr.)*, 2000, **10**, 289.